AIMS Mathematics, 10(3): 6069–6101.
DOI: 10.3934/math.2025277
Received: 29 December 2024
Revised: 03 March 2025
Accepted: 06 March 2025
Published: 19 March 2025

http://www.aimspress.com/journal/Math

Research article

A discrete extension of the Xgamma random variable: mathematical framework, estimation methods, simulation ranking, and applications to radiation biology and industrial engineering data

Mohamed S. Algolam[1], Mohamed S. Eliwa[2], Mohamed El-Dawoody[3] and Mahmoud El-Morshedy[3,*]

[1] Department of Mathematics, College of Science, University of Ha'il, Ha'il 2440, Saudi Arabia

[2] Department of Statistics and Operations Research, College of Science, Qassim University, Saudi Arabia

[3] Department of Mathematics, College of Science and Humanities in Al-Kharj, Prince Sattam Bin Abdulaziz University, Al-Kharj 11942, Saudi Arabia

* **Correspondence:** Email: m.elmorshedy@psau.edu.sa.

Abstract: Count data modeling and its practical applications have garnered significant attention in recent research, owing to its relevance in a wide range of fields. This study specifically explores a novel discrete distribution characterized by two parameters, which is derived using the survival discretization method. The statistical properties of this distribution are thoroughly explained in closed forms, with several key mathematical attributes also derived. These characteristics underscore the distribution's effectiveness in modeling data that exhibit (right-skewed) asymmetry and have extended heavy tails, making it particularly suitable for such real-world applications. Furthermore, the failure rate function corresponding to this distribution is particularly appropriate for scenarios characterized by an increasing or bathtub-shaped failure rate over time. The model is also highly versatile, offering valuable insights into probabilistic modeling for datasets that display over dispersion, under dispersion, or equi dispersion. The study introduces several estimation techniques, including the maximum product of spacings, Anderson–Darling, right–tail Anderson–Darling, maximum likelihood estimation, least squares, weighted least squares, Cramer–Von–Mises, and percentile methods. Each of these methods is explained in detail, providing a comprehensive understanding of their application. A ranking simulation study is conducted to evaluate the performance of these estimators across varying sample sizes, using ranking techniques to identify the most effective estimator in different scenarios. The analysis of real-world datasets from biotechnology and industrial engineering further demonstrates the practical utility and relevance of the proposed model. The results highlight the model's ability to offer accurate and insightful analyses, reinforcing its significance in count data modeling and its wide-ranging applications.

Keywords: statistical model; survival discretization technique; failure analysis; estimation methods; simulation; statistics and numerical data
Mathematics Subject Classification: 62E99, 62E15

1. Introduction

Count data modeling is a fundamental aspect of statistical analysis, providing essential insights across a wide range of scientific fields. Count data consist of non–negative integers that reflect the frequency of events within a given unit of measurement, making them crucial in disciplines such as epidemiology, ecology, finance, social sciences, biotechnology, and engineering. These data help identify patterns and trends, enabling researchers to better understand various real–world phenomena. For example, in epidemiology, count data are used to track the number of disease cases within a population over time, aiding in the study of disease prevalence, transmission patterns, and the effectiveness of public health interventions. In ecology, they play a key role in assessing species' populations, biodiversity, and conservation efforts. By accurately modeling count data, researchers can make informed decisions and develop strategies to address complex challenges in different domains. In finance, counts such as trading volumes or the frequency of specific market events inform risk assessments and portfolio management. In the social sciences, count data play a crucial role in studies of survey responses [1] and voting patterns [2]. Similarly, in biotechnology and engineering, count data are utilized to analyze occurrences such as gene expression levels [3], manufacturing defects [4], or system failures [5], aiding in advancements and optimization within these fields [6].

However, count data pose distinct challenges for analysis. Overdispersion is a common issue, where the observed variance exceeds the expected value under standard Poisson models, necessitating the use of more flexible models such as the negative binomial distribution. Zero–inflation, another challenge, occurs when datasets contain an excess of zero counts, which requires specific techniques to avoid bias. Additionally, count data may exhibit complex dependency structures, including spatial or temporal correlations, which complicates the development and selection of models.

Given the fundamental importance of discrete probability models in capturing such patterns, we have developed and thoroughly investigated a new discrete probability distribution, building upon our previous survey work to address these specific challenges. This newly introduced model serves as the discrete counterpart to an extension of the xgamma (Exg) distribution. The Exg distribution has gained significant prominence across various domains, such as reliability analysis, survival modeling, and risk assessment, due to its flexibility and ability to capture a broad range of data patterns. It is particularly valued for its capacity to model right-skewed and heavy-tailed data, making it highly effective in representing diverse real-world phenomena. By integrating features from multiple distributions, the Exg model offers researchers a powerful tool for modeling complex datasets, facilitating a more profound understanding of the underlying mechanisms that drive observed events. For further details and an in-depth exploration of the Exg distribution, please refer to [7]. A random variable Z is said to follow the Exg distribution when its reliability function (RF), say $R(z;\zeta,\tau)$, and

probability density function (PDF), say $g(z;\zeta,\tau)$, can be expressed as follows:

$$R(z;\zeta,\tau) = \frac{\zeta\tau^2 e^{-\tau z}}{\zeta+\tau^2}\eta(z;\zeta,\tau);\ z>0, \tag{1.1}$$

and

$$g(z;\zeta,\tau) = \frac{\tau^3}{\zeta+\tau^2}\left[1+\frac{\zeta z^2}{2}\right]e^{-\tau z};\ z>0, \tag{1.2}$$

respectively, where

$$\eta(z;\zeta,\tau) = \frac{1}{\zeta}+\frac{1}{\tau^2}+\frac{z}{\tau}+\frac{z^2}{2}; \zeta>0,\ \tau>0.$$

Using survival discretization techniques, a discrete analog of an extension to the xgamma (DExg) distribution can be derived. This technique is a statistical method designed to transform continuous probability distributions, like the Exg distribution, into discrete forms that are more applicable for real-world scenarios. Since real-world data are frequently recorded in discrete units or intervals, survival discretization is particularly useful. Through this process, the probability mass function (PMF) can be obtained as follows:

$$\Pr(Z=z;.) = R(z;.) - R(z+1;.);\ z=0,1,2,3,.... \tag{1.3}$$

For a more detailed explanation of the survival discretization approach, refer to Roy [8]. Several discrete distributions based on the discrete survival function have been proposed and studied, including the discrete Burr–Hatke [9], discrete Pareto [10], discrete inverse Rayleigh [11], discrete exponentiated generalized family of distributions [12], a novel version of geometric distribution [13], discrete inverse Weibull [14], discrete Burr–XII [10], discrete Lindley [15], new discrete extended Weibull [16], new Poisson–weighted exponential [17], discrete generalized geometric [18], discrete Gompertz [19], discrete generalized exponential Type II [20], discrete Ramos–Louzada [21], and the two-parameter discrete Lindley [22]. While numerous discrete probability models exist in the statistical literature, the growing complexity of daily generated data underscores the need for more flexible discrete distributions to effectively tackle these challenges. This is particularly crucial in cases that require closed-form expressions for statistical and reliability properties, as well as for addressing issues such as dispersion, heavy tails, irregular failure rates, outliers, and kurtosis, where traditional models often fall short. As a result, the DExg model has been proposed and thoroughly examined for its unique features, which allow it to capture a wide range of data behaviors and overcome the limitations of conventional models. The motivations for this can be summarized as follows:

- To introduce a discrete distribution with straightforward and closed-form expressions for essential properties, including the PMF, RF, moments, and related measures, facilitating efficient data modeling and fitting.
- To design a discrete model that effectively fits practical datasets, such as those arising in industrial or mortality studies, while accommodating bathtub–shaped or increasing failure rates and ensuring a non–decreasing failure rate function for realistic applications.
- To develop a flexible model that is capable of fitting diverse data types, including equi–dispersed, over–dispersed, and under–dispersed datasets, as well as distributions with positive skewness or leptokurtic characteristics.

- To propose a robust model specifically tailored for the analysis and fitting of count data, outperforming the existing discrete models commonly used in statistical applications.

The structure of this article is organized as follows: Section 2 introduces the DExg distribution, developed using the survival discretization approach. Section 3 explores the statistical properties of the distribution in detail. Section 4 addresses the estimation of distribution parameters through various methodologies. In Section 5, a comprehensive simulation study is conducted, incorporating ranking techniques. Section 6 demonstrates the versatility of the DExg distribution through analyses of multiple datasets. Finally, Section 7 concludes with a summary of the key findings and outlines directions for future research.

2. Structural characteristics of the DExg distribution

Applying Eqs (1.1) and (1.3), the cumulative distribution function (CDF) and its associated PMF are expressed as follows:

$$F(z;\zeta,\tau) = 1 - \frac{\zeta\tau^2 e^{-\tau(z+1)}}{\zeta+\tau^2}\eta\left(z+1;\zeta,\tau\right);\ z \in \mathbb{N}_{0,} \tag{2.1}$$

and

$$\Pr\left(Z=z;\zeta,\tau\right) = \frac{\zeta\tau^2}{\zeta+\tau^2}\left[\eta\left(z;\zeta,\tau\right) - e^{-\tau}\eta\left(z+1;\zeta,\tau\right)\right]e^{-\tau z};\ z \in \mathbb{N}_{0,} \tag{2.2}$$

respectively. The behavior of the PMF under various conditions is given as

$$\Pr\left(Z=z;\zeta,\tau\right) = \begin{cases} (1-e^{-\tau})e^{-\tau z} & ;\ \ \zeta \to 0 \\ (\frac{1}{2}\tau^2 z^2 + \tau z + 1)e^{-\tau z} - \left(\tau^2\left[\frac{1}{2}z^2 + z + \frac{1}{2}\right] + \tau[z+1] + 1\right)e^{-\tau(z+1)} & ;\ \ \zeta \to \infty \\ 0 & ;\ \ \tau \to 0 \\ \left[(\tau^2+\zeta) - \left(\frac{1}{2}\zeta\tau^2 + \zeta\tau + \tau^2 + \zeta\right)e^{-\tau}\right]\left[\tau^2+\zeta\right]^{-1} & ;\ \ z \to 0. \end{cases} \tag{2.3}$$

Figure 1 displays the PMF plots for different values of the parameter ζ and τ.

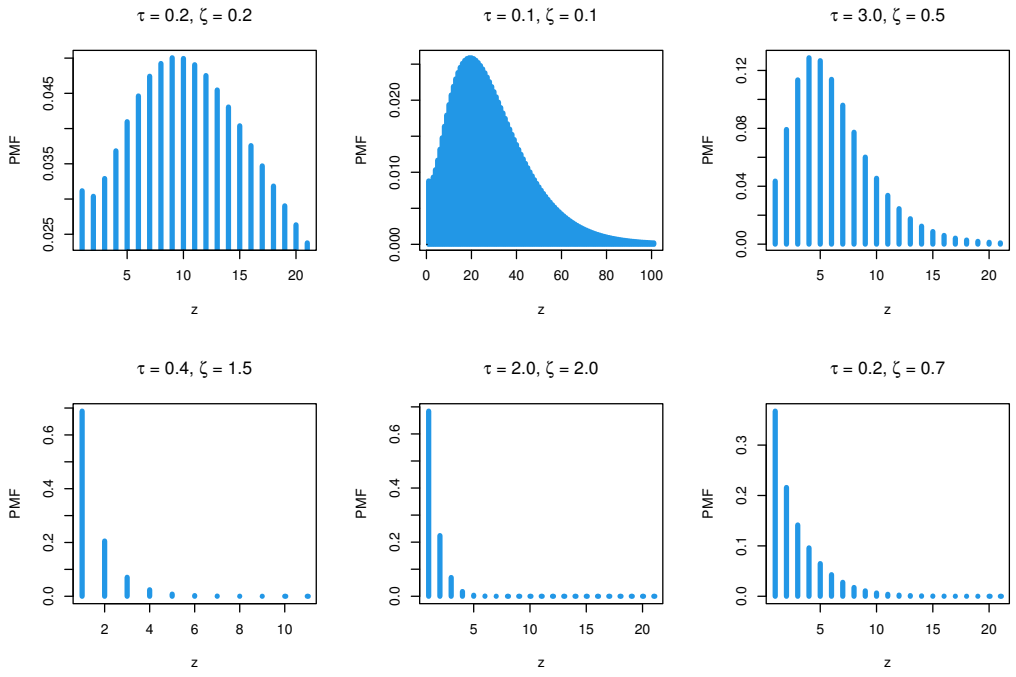

Figure 1. The PMF plots of the DExg model.

It is important to highlight that the PMF is particularly effective for modeling data with a unimodal shape. Additionally, it demonstrates its versatility by effectively analyzing asymmetric, positively skewed, and heavy-tailed data, making it well-suited for capturing a wide range of data patterns. The hazard rate function (HRF) of the DExg model can be expressed as

$$h(z;\zeta,\tau) = \frac{\eta(z;\zeta,\tau) - e^{-\tau}\eta(z+1;\zeta,\tau)}{e^{-\tau}\eta(z;\zeta,\tau)};\ z \in \mathbb{N}_0. \tag{2.4}$$

The reversed hazard rate function (RHRF) can be given as

$$r(z;\zeta,\tau) = \frac{\zeta\tau^2\left[\eta(z;\zeta,\tau) - e^{-\tau}\eta(z+1;\zeta,\tau)\right]e^{-\tau z}}{\left[\zeta+\tau^2-\zeta\tau^2 e^{-\tau(z+1)}\eta(z+1;\zeta,\tau)\right]};\ z \in \mathbb{N}_0. \tag{2.5}$$

The HRF represents the likelihood of an item's failure at a specific age z, and it forms part of the broader hazard function equation. This equation assesses the probability that an item, having survived up to a certain time t, will continue to last beyond that point. In essence, it quantifies the chance that an item surviving at one moment will persist to the next. The hazard rate is particularly relevant for non-repairable items and is often referred to as the failure rate. Its importance spans the design of secure systems in various fields, including commerce, engineering, finance, insurance, and regulatory industries. Mathematically, it is expressed as the ratio of the PMF to the corresponding RF. On the other hand, the RHRF for a random lifetime is defined as the ratio of the PMF to the CDF. This concept is crucial in analyzing censored data and finds applications in areas such as forensic science. Figures 2 and 3 shows the HRF and RHRF plots for different values of the parameters ζ and τ.

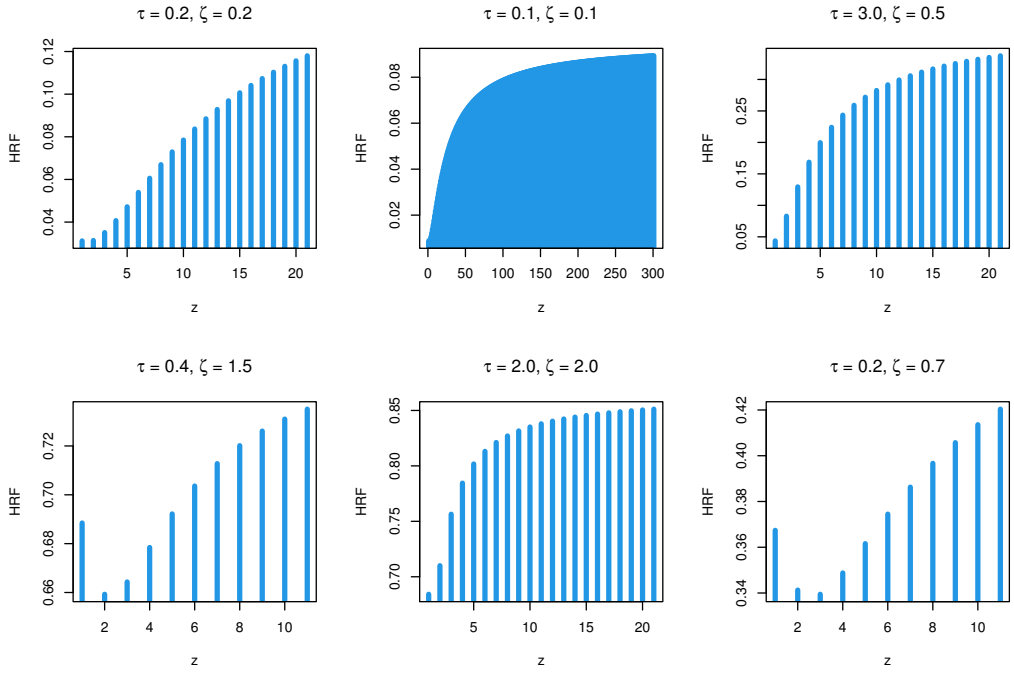

Figure 2. The HRF plots of the DExg distribution.

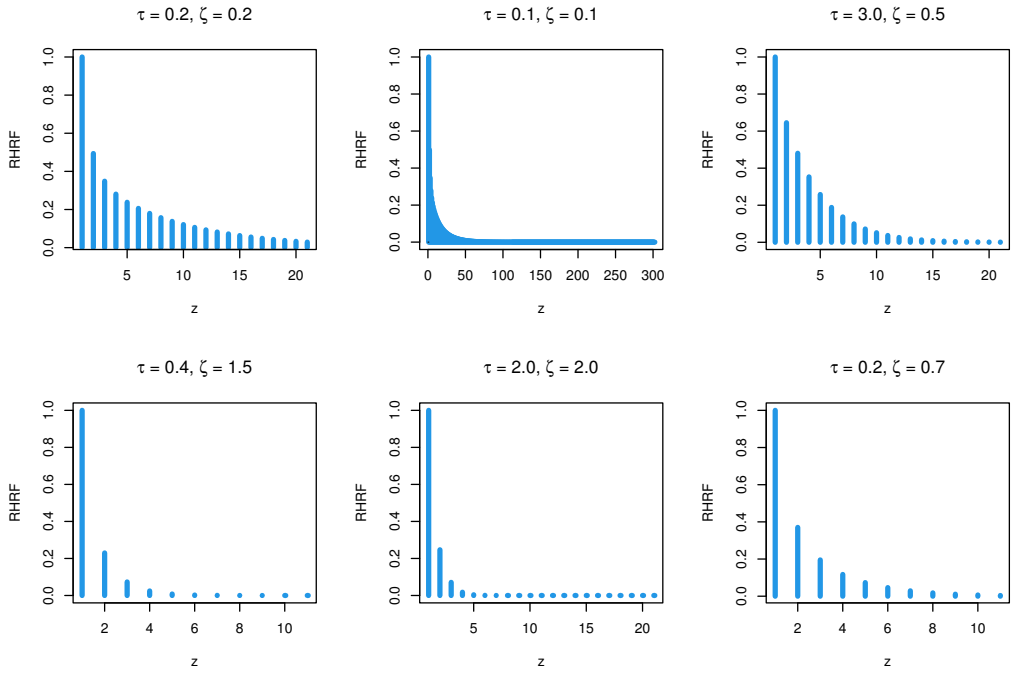

Figure 3. The RHRF plots of the DExg distribution.

3. Some statistical features

3.1. Order statistics

Consider a situation where we have a collection of n random variables, represented as $Z_1, Z_{2,}..., Z_n$, arranged in non–decreasing order, such that $Z_{1:n} \leq Z_{2:n} \leq ... \leq Z_{n:n}$. In the realm of order statistics, it is essential to understand that there are no restrictions on whether these X_i values are independent or identically distributed. Nevertheless, many established results related to order statistics are derived on the basis of the classical assumption that the X_i values are independent and identically distributed. For the DExg distribution, the CDF of the ith order statistic can be expressed as

$$\begin{aligned} F_{i:n}(z;\zeta,\tau) &= \sum_{k=i}^{n}\binom{n}{k}\left[F_i(z;\zeta,\tau)\right]^k\left[1-F_i(z;\zeta,\tau)\right]^{n-k} \\ &= \sum_{k=i}^{n}\sum_{j=0}^{n-k}\Phi_m^{(n,k)}\left[1-\frac{\zeta\tau^2 e^{-\tau(z+1)}}{\zeta+\tau^2}\eta(z+1;\zeta,\tau)\right]^{k+j}, \end{aligned}$$

where $\Phi_m^{(n,k)} = (-1)^j\binom{n}{k}\binom{n-k}{j}$. Moreover, the associated PMF of the ith order statistic is given by

$$\begin{aligned} f_{i:n}(z;\zeta,\tau) &= F_{i:n}(z;\zeta,\tau) - F_{i:n}(z-1;\zeta,\tau) \\ &= \sum_{k=i}^{n}\sum_{j=0}^{n-k}\Theta_{(m,j)}^{(n,k)}(\zeta,\tau)\left[\left[\eta(z;\zeta,\tau) - e^{-\tau}\eta(z+1;\zeta,\tau)\right]e^{-\tau z}\right]^{k+j}, \end{aligned} \tag{3.1}$$

where

$$\Theta_{(m,j)}^{(n,k)}(\zeta,\tau) = \Phi_m^{(n,k)}\left(\frac{\zeta\tau^2}{\zeta+\tau^2}\right)^{k+j}.$$

Thus, the rth moments of $Z_{i:n}$ can be expressed as

$$\mu_{i:n}^{(r)} = E\left(Z_{i:n}^r\right) = \sum_{z=0}^{\infty}\sum_{k=i}^{n}\sum_{j=0}^{n-k} z^r\,\Theta_{(m,j)}^{(n,k)}(\zeta,\tau)\left[\left[\eta(z;\zeta,\tau) - e^{-\tau}\eta(z+1;\zeta,\tau)\right]e^{-\tau z}\right]^{k+j}. \tag{3.2}$$

Moreover, since the support of the DExg distribution is $\mathbb{N}_0$, therefore, $\mu_{1:n}^{(1)}$, $\mu_{n:n}^{(1)}$, $\mu_{1:n}^{(2)}$, and $\mu_{n:n}^{(2)}$ can be directly derived utilizing $F_{i:n}(z;\zeta,\tau)$ (see Arnold et al. [23]) as follows

$$\begin{aligned} \mu_{1:n}^{(1)} &= \sum_{z=0}^{\infty}\left[\frac{\zeta\tau^2 e^{-\tau(z+1)}}{\zeta+\tau^2}\eta(z+1;\zeta,\tau)\right]^n, \\ \mu_{n:n}^{(1)} &= \sum_{z=0}^{\infty}\left[1-\left\{1-\frac{\zeta\tau^2 e^{-\tau(z+1)}}{\zeta+\tau^2}\eta(z+1;\zeta,\tau)\right\}^n\right], \\ \mu_{1:n}^{(2)} &= 2\sum_{z=0}^{\infty} z\left[\frac{\zeta\tau^2 e^{-\tau(z+1)}}{\zeta+\tau^2}\eta(z+1;\zeta,\tau)\right]^n + \mu_{1:n}^{(1)}, \\ \mu_{n:n}^{(2)} &= 2\sum_{z=0}^{\infty} z\left[1-\left\{1-\frac{\zeta\tau^2 e^{-\tau(z+1)}}{\zeta+\tau^2}\eta(z+1;\zeta,\tau)\right\}^n\right] + \mu_{n:n}^{(1)}, \end{aligned}$$

where

$$\eta(z+1;\zeta,\tau)=\frac{1}{\zeta}+\frac{1}{\tau^2}+\frac{z+1}{\tau}+\frac{(z+1)^2}{2};\zeta>0,\ \tau>0.$$

According to $\mu^{(1)}_{1:n}$, $\mu^{(1)}_{n:n}$, $\mu^{(2)}_{1:n}$, and $\mu^{(2)}_{n:n}$, $\sigma^2_{1,1:n}$ and $\sigma^2_{n,n:n}$ can be reported. The numerical results provide insights into the behavior of the order statistics' expectations and variances for different values of n and τ. As n increases, $\mu^{(1)}_{1:n}$ decreases, indicating that the smallest order statistic shifts towards lower values. In contrast, $\mu^{(1)}_{n:n}$ remains close to 49, suggesting that the maximum order statistic stabilizes at an upper bound. The second moments, $\mu^{(2)}_{1:n}$ and $\mu^{(2)}_{n:n}$, follow similar trends, with the former decreasing and the latter maintaining a high magnitude. The variances, $\sigma^2_{1,1:n}$ and $\sigma^2_{n,n:n}$, exhibit an interesting pattern: $\sigma^2_{1,1:n}$ is very small, implying that the smallest order statistic is highly concentrated, while $\sigma^2_{n,n:n}$ is relatively large but decreases slightly as n grows, signifying increased stability in the maximum order statistic. These results highlight the impact of the sample size and distribution parameters on the dispersion and expectation of extreme order statistics.

3.2. Statistical moments and associated notions

In probability theory and statistical analysis, several key functions and measures are employed to characterize the behavior of random variables. The moment generating function (MGF), defined as $M_Z(t;.)=E(e^{tZ})$, serves to encapsulate all moments of a distribution, enabling the extraction of higher-order moments through differentiation with respect to t at $t=0$. This function is instrumental in deriving essential quantities like the expectation and variance, which provide insight into the central tendency and dispersion of a random variable, respectively. Moreover, skewness and kurtosis, which are higher-order moments obtained from the MGF, characterize the asymmetry and the tail behavior (or peakedness) of the distribution.

In the case of discrete random variables, the probability generating function (PGF), defined as $G_Z(s;.)=E(s^Z)$ (where s is a real number) offers a concise representation of the PMF and facilitates the derivation of probabilities and moments. The PGF is particularly valuable for studying integer-valued random variables, focusing on the distribution of outcomes. For the DExg distribution, both the MGF and PGF can be expressed in explicit forms, though their expressions may be intricate. Special cases, such as when the parameter ζ approaches zero or infinity, yield simplified representations of these functions, offering valuable insights into the underlying probabilistic structure. The MGF of the DExg distribution can be formulated as

$$M_Z(t;\zeta,\tau)=\begin{cases}\frac{1-e^{\tau}}{e^{t}-e^{\tau}} & ;\quad \zeta\to 0\\ \\ \frac{\Upsilon(t;\tau)}{2\left(e^{3t}-3e^{\tau+2t}+3e^{2\tau+t}-e^{3\tau}\right)} & ;\quad \zeta\to\infty,\end{cases}$$

where

$$\begin{aligned}\Upsilon(t;\tau)=&\tau^2\left(-e^{\tau+2t}-e^{2\tau+t}+e^{\tau+t}+e^{2\tau}\right)+2\tau\left(e^{\tau+2t}-e^{2\tau+t}-e^{\tau+t}+e^{2\tau}\right)\\&+2\left(2e^{2\tau+t}-e^{\tau+2t}-e^{3\tau}+e^{2t}-2e^{\tau+t}+e^{2\tau}\right).\end{aligned}$$

The PGF can be derived from the MGF by substituting $s=e^t$. Furthermore, the first four moments of

the DExg distribution can be proposed as

$$E(Z) = \begin{cases} \frac{1}{e^{\tau}-1} & ; \quad \zeta \to 0 \\ \frac{\tau^2(e^{\tau}+1)e^{\tau}+2\tau(e^{\tau}-1)e^{\tau}+2\left(e^{2\tau}-e^{\tau}+1\right)}{2\left(e^{3t}-3e^{2\tau}+3e^{\tau}-1\right)} & ; \quad \zeta \to \infty, \end{cases}$$

$$E(Z^2) = \begin{cases} \frac{e^{\tau}+1}{e^{2\tau}-2e^{\tau}+1} & ; \quad \zeta \to 0 \\ \frac{\tau^2\left(e^{2\tau}+8e^{\tau}+3\right)e^{\tau}+2\tau\left(e^{2\tau}+2e^{\tau}-3\right)e^{\tau}+2\left(e^{3\tau}-e^{2\tau}-e^{\tau}+1\right)}{2\left(e^{4\tau}-4e^{3\tau}+6e^{2t}-4e^{\tau}+1\right)} & ; \quad \zeta \to \infty, \end{cases}$$

$$E(Z^3) = \begin{cases} \frac{e^{2\tau}+4e^{\tau}+1}{e^{3t}-3e^{2\tau}+3e^{\tau}-1} & ; \quad \zeta \to 0 \\ \frac{\tau^2\left(e^{3\tau}+23e^{2\tau}+41e^{\tau}+7\right)e^{\tau}+2\tau\left(e^{3\tau}+9e^{2\tau}-3e^{\tau}-7\right)e^{\tau}+2\left(e^{4\tau}+2e^{3\tau}-6e^{2\tau}+2e^{\tau}+1\right)}{2\left(e^{5\tau}-5e^{4\tau}+10e^{3\tau}-10e^{2t}+5e^{\tau}-1\right)} & ; \quad \zeta \to \infty, \end{cases}$$

$$E(Z^4) = \begin{cases} \frac{e^{3\tau}+11e^{2\tau}+11e^{\tau}+1}{e^{4\tau}-4e^{3\tau}+6e^{2t}-4e^{\tau}+1} & ; \quad \zeta \to 0 \\ \frac{\tau^2\left(e^{4\tau}+54e^{3\tau}+240e^{2\tau}+170e^{\tau}+15\right)e^{\tau}+2\tau\left(e^{4\tau}+24e^{3\tau}+30e^{2\tau}-40e^{\tau}-15\right)e^{\tau}+2\left(e^{5\tau}+9e^{4\tau}-10e^{3\tau}-10e^{2\tau}+9e^{\tau}+1\right)}{2\left(e^{6\tau}-6e^{5\tau}+15e^{4\tau}-20e^{3\tau}+15e^{2\tau}-6e^{t}+1\right)} & ; \quad \zeta \to \infty. \end{cases}$$

Table 1 presents various statistical measures for different combinations of the parameters ζ and τ.

Table 1. Numerical descriptors for characterizing the DExg distribution.

Measure	$\zeta \downarrow \tau \rightarrow$	0.1	0.3	0.5	10.0	20.0	30.0
$E(Z)$	0.05	26.144	5.230	2.201	47×10^{-5}	2.1×10^{-9}	9.6×10^{-14}
	0.5	28.980	8.486	4.180	58×10^{-5}	2.6×10^{-9}	1.2×10^{-13}
	1.5	29.402	9.123	4.934	85×10^{-5}	3.7×10^{-9}	1.7×10^{-13}
Variance(Z)	0.05	323.296	29.152	7.455	47×10^{-5}	2.1×10^{-9}	9.5×10^{-14}
	0.5	310.903	35.704	12.844	58×10^{-5}	2.6×10^{-9}	1.1×10^{-13}
	1.5	297.979	34.506	12.837	85×10^{-5}	3.7×10^{-9}	1.6×10^{-13}
Variability index(Z)	0.05	12.365	5.573	3.386	1.000	1.000	0.99999
	0.5	10.728	4.207	3.072	1.000	1.000	0.99999
	1.5	10.134	3.781	2.601	1.000	1.000	0.99999
Skewness(Z)	0.05	1.077	1.579	1.991	146.244	21729.74	3.2×10^{6}
	0.5	1.084	1.082	1.179	130.254	19509.592	2.9×10^{6}
	1.5	1.261	1.103	1.084	108.062	16318.50	2.4×10^{6}
Kurtosis(Z)	0.05	4.694	6.222	8.450	21392.61	4.7×10^{8}	1.0×10^{13}
	0.5	4.7304	4.744	4.854	16972.09	3.8×10^{8}	8.4×10^{12}
	1.5	4.580	4.863	4.747	11683.34	2.6×10^{8}	5.9×10^{12}

As τ increases, the expected value and variance of Z decrease significantly, with higher values of τ leading to near-zero values, indicating that the distribution becomes more concentrated around its mean. The variability index decreases similarly, stabilizing near 1 for a large τ, reflecting reduced relative dispersion. Conversely, skewness and kurtosis grow exponentially with increasing values of τ,

showing that the distribution becomes highly asymmetric with heavy tails and large outliers at higher τ values. Emphasizing the pivotal role that ζ and τ play in shaping the distribution's central tendency, dispersion, and overall form, the DExg distribution proves particularly useful for modeling data that are over-dispersed, under-dispersed, or equi-dispersed. This distribution is especially effective in handling right-skewed data with a leptokurtic shape, making it ideal for discussing complex real-world scenarios where skewness and high kurtosis are prevalent.

3.3. Entropy in information theory

Entropy is a crucial measure in information theory and statistical modeling, quantifying the uncertainty or randomness of a probability distribution. In the context of the DExg distribution, entropy can be particularly useful for evaluating the complexity of data generated by the model, assessing the model selection criteria, and optimizing information-based decision-making processes. For example, in reliability analysis, entropy helps quantify the unpredictability of failure times, while in actuarial sciences, it aids in risk assessments. For a discrete random variable Z that takes values from the set Ω, and is distributed according to p: $\Omega \to [0, 1]$, the residual entropy of the variable Z and its cumulative expression can be listed, respectively, as follows:

$$\mathcal{I}(z; .) = -\sum_{z=0}^{\infty} F(z; .) \log(F(z; .)),$$

and

$$C\mathcal{I}(z; .) = -\sum_{z=0}^{\infty} (1 - F(z; .)) \log(1 - F(z; .)).$$

By utilizing algebraic techniques (the Taylor series for $\log(1 - W); |W| < 1$) with respect to the DExg distribution, we can derive

$$\begin{aligned}\mathcal{I}(Z) &= -\sum_{z=0}^{\infty} \left[1 - \frac{\zeta\tau^2 e^{-\tau(z+1)}}{\zeta + \tau^2}\eta(z + 1; \zeta, \tau))\right] \log\left[1 - \frac{\zeta\tau^2 e^{-\tau(z+1)}}{\zeta + \tau^2}\eta(z + 1; \zeta, \tau)\right] \\ &= \sum_{z=0}^{\infty}\sum_{n=1}^{\infty} \frac{1}{n}\left[1 - \frac{\zeta\tau^2 e^{-\tau(z+1)}}{\zeta + \tau^2}\eta(z + 1; \zeta, \tau))\right]\left[\frac{\zeta\tau^2 e^{-\tau(z+1)}}{\zeta + \tau^2}\eta(z + 1; \zeta, \tau)\right]^n,\end{aligned}$$

and

$$C\mathcal{I}(Z) = -\frac{\zeta\tau^2}{\zeta + \tau^2}\sum_{z=0}^{\infty}\left[e^{-\tau(z+1)}\eta(z + 1; \zeta, \tau))\right] \log\left[\frac{\zeta\tau^2 e^{-\tau(z+1)}}{\zeta + \tau^2}\eta(z + 1; \zeta, \tau)\right].$$

Algebraic methods, particularly the Taylor series expansion for $\log(1 - W)$ with $|W| < 1$, are applied to streamline the mathematical analysis of the DExg distribution. This approach provides several advantages, including analytical simplicity by making complex expressions more manageable, improved numerical computation through infinite series approximations, and stable convergence properties that ensure the validity of the derived results. Additionally, the Taylor series expansion facilitates the generalization and approximation of key statistical measures, such as entropy and information indices, enhancing interpretability and practical implementation. By leveraging these techniques, this study strengthens both the theoretical foundation and applied relevance of the DExg

distribution in statistical modeling. The Rényi entropy of the random variable Z, derived using the generalized binomial expansion, is defined as

$$I_R(Z;\omega) = \frac{1}{1-\omega}\log\left(\left[\frac{\zeta\tau^2}{\zeta+\tau^2}\right]^{\omega}\sum_{z=0}^{\infty}\left[\eta\left(z;\zeta,\tau\right)-e^{-\tau}\eta\left(z+1;\zeta,\tau\right)\right]^{\omega}e^{-\omega\tau z}\right), \tag{3.3}$$

where $\omega > 0$ and $\omega \neq 1$. Shannon entropy can be computed as a specific instance of Rényi entropy when the parameter ω approaches 1. Table 2 presents numerical calculations for the entropies reported in this section.

Table 2. Entropies using the DExg distribution.

Measure	$\zeta \downarrow \tau \rightarrow$	0.1	0.3	0.5	0.7	0.9
$\mathcal{I}(Z)$	0.5	5.7992	1.9862	1.1384	0.7291	0.4937
	0.7	5.7825	1.9819	1.1651	0.7701	0.5344
	0.9	5.7726	1.9754	1.1768	0.7942	0.5621
$C\mathcal{I}(Z)$	0.5	7.4406	2.5435	1.5304	1.0552	0.7714
	0.7	7.4298	2.5294	1.5345	1.0773	0.8024
	0.9	7.4056	2.5193	1.5327	1.0870	0.8201
$I_R(Z;1.5)$	0.5	0.2633	0.4499	0.6040	0.7688	0.9347
	0.7	0.2637	0.4496	0.5909	0.7374	0.8898
	0.9	0.2639	0.4501	0.5850	0.7192	0.8601

The data indicate that both τ and ζ influence these measures. Notably, $\mathcal{I}(Z)$ and $C\mathcal{I}(Z)$ generally decrease as τ increases for each ζ, with $C\mathcal{I}(Z)$ being consistently larger than $\mathcal{I}(Z)$. The effect of ζ becomes more noticeable at higher τ values. $I_R(Z;1.5)$ shows the opposite trend, increasing as τ increases, with minimal variation across ζ values for small values of τ but more divergence at higher τ values.

3.4. The (reversed) hazard rate function for two-component parallel and series systems

The HRF plays a crucial role in reliability analysis, particularly for two-component systems arranged in parallel and series configurations. In a two-component parallel system, the system fails only when both components fail, leading to an overall hazard rate that reflects the redundancy and increased reliability provided by the parallel structure. Conversely, in a two-component series system, the system fails if either component fails, resulting in a higher overall hazard rate due to the system's vulnerability to single-point failures. Understanding the HRF for these configurations is essential for modeling and optimizing systems' reliability in various practical applications. Suppose that T_1 and T_2 are two independent DExg random variables with the parameters (ζ_1,τ_1) and (ζ_2,τ_2), respectively. Then, the HRF of $W = \min(T_1,T_2)$ can be formulated as

$$\begin{aligned} h_W(z;\xi) &= \frac{\Pr(\min(T_1,T_2)=z)}{\Pr(\min(T_1,T_2)\geq z)} \\ &= \frac{\Pr(\min(T_1,T_2)\geq z)-\Pr(\min(T_1,T_2)\geq z+1)}{\Pr(\min(T_1,T_2)\geq z)} \end{aligned}$$

$$= \frac{\Pr(T_1 \geq z)\Pr(T_2 \geq z) - \Pr(T_1 \geq z+1)\Pr(T_2 \geq z+1)}{\Pr(T_1 \geq z)\Pr(T_2 \geq z)},$$

then

$$h_W(z;\xi) = \frac{\eta(z;\zeta_1,\tau_1) - e^{-\tau_1}\eta(z+1;\zeta_1,\tau_1)}{e^{-\tau_1}\eta(z;\zeta_1,\tau_1)} + \frac{\eta(z;\zeta_2,\tau_2) - e^{-\tau_2}\eta(z+1;\zeta_2,\tau_2)}{e^{-\tau_2}\eta(z;\zeta_2,\tau_2)} - \frac{\left[\eta(z;\zeta_1,\tau_1) - e^{-\tau_1}\eta(z+1;\zeta_1,\tau_1)\right]\left[\eta(z;\zeta_2,\tau_2) - e^{-\tau_2}\eta(z+1;\zeta_2,\tau_2)\right]}{\eta(z;\zeta_1,\tau_1)\,\eta(z;\zeta_2,\tau_2)\,e^{-(\tau_1+\tau_2)}},$$

where $\xi = (\zeta_1, \tau_1, \zeta_2, \tau_2)$ and $z \in \mathbb{N}_0$. Since the HRF of T_1 and T_2 is increasing, then the HRF of W is also increasing. Similarly, the HRF of $W^* = \max(T_1, T_2)$ can be given as

$$h_{W^*}(z;\xi) = 1 - \frac{1 - \left\{1 - \frac{\zeta_1\tau_1^2 e^{-\tau_1(z+1)}}{\zeta_1+\tau_1^2}\eta(z+1;\zeta_1,\tau_1)\right\}\left\{1 - \frac{\zeta_2\tau_2^2 e^{-\tau_2(z+1)}}{\zeta_2+\tau_2^2}\eta(z+1;\zeta_2,\tau_2)\right\}}{1 - \left\{1 - \frac{\zeta_1\tau_1^2 e^{-\tau_1(z+1)}}{\zeta_1+\tau_1^2}\eta(z;\zeta_1,\tau_1)\right\}\left\{1 - \frac{\zeta_2\tau_2^2 e^{-\tau_2(z+1)}}{\zeta_2+\tau_2^2}\eta(z;\zeta_2,\tau_2)\right\}}.$$

The HRF of the random variable W^* is also increasing. On the other hand, the RHRF of W and W^* can be reported as

$$r_W(z;\xi) = 1 - \frac{1 - \zeta_1\zeta_2\tau_1^2\tau_2^2\left(\zeta_1+\tau_1^2\right)^{-1}\left(\zeta_2+\tau_2^2\right)^{-1} e^{-(z+1)(\tau_1+\tau_2)}\eta(z;\zeta_1,\tau_1)\,\eta(z;\zeta_2,\tau_2)}{1 - \zeta_1\zeta_2\tau_1^2\tau_2^2\left(\zeta_1+\tau_1^2\right)^{-1}\left(\zeta_2+\tau_2^2\right)^{-1} e^{-(z+1)(\tau_1+\tau_2)}\eta(z+1;\zeta_1,\tau_1)\,\eta(z+1;\zeta_2,\tau_2)},$$

and

$$r_{W^*}(z;\xi) = \frac{\zeta_1\tau_1^2\left[\eta(z;\zeta_1,\tau_1) - e^{-\tau_1}\eta(z+1;\zeta_1,\tau_1)\right]e^{-\tau_1 z}}{\left[\zeta_1+\tau_1^2 - \zeta_1\tau_1^2 e^{-\tau_1(z+1)}\eta(z+1;\zeta_1,\tau_1)\right]} + \frac{\zeta_2\tau_2^2\left[\eta(z;\zeta_2,\tau_2) - e^{-\tau_2}\eta(z+1;\zeta_2,\tau_2)\right]e^{-\tau_2 z}}{\left[\zeta_2+\tau_2^2 - \zeta_2\tau_2^2 e^{-\tau_2(z+1)}\eta(z+1;\zeta_2,\tau_2)\right]} - \left\{\frac{\left[\zeta_1\tau_1^2\left[\eta(z;\zeta_1,\tau_1) - e^{-\tau_1}\eta(z+1;\zeta_1,\tau_1)\right]e^{-\tau_1 z}\right]\left[\zeta_2\tau_2^2\left[\eta(z;\zeta_2,\tau_2) - e^{-\tau_2}\eta(z+1;\zeta_2,\tau_2)\right]e^{-\tau_2 z}\right]}{\left[\zeta_1+\tau_1^2 - \zeta_1\tau_1^2 e^{-\tau_1(z+1)}\eta(z+1;\zeta_1,\tau_1)\right]\left[\zeta_2+\tau_2^2 - \zeta_2\tau_2^2 e^{-\tau_2(z+1)}\eta(z+1;\zeta_2,\tau_2)\right]}\right\}.$$

By analyzing the HRF and RHRF, engineers and analysts can optimize a system's performance and plan maintenance strategies based on actual operational time before failure or a failure's occurrence. The HRF and RHRF of the DExg distribution play a crucial role in understanding systems' reliability, particularly in two-component parallel and series systems. The HRF is essential for evaluating series systems, where the failure of a single component results in the system's failure, making it a key tool for identifying weak links. The DExg distribution's flexibility in modeling bathtub-shaped and increasing failure rates makes it well-suited for systems prone to early-life failures or gradual wear-out. Conversely, the RHRF is particularly valuable for analyzing parallel systems, which fail only when all components fail. It provides insights into the expected operational lifetime of a system before failure, making it especially useful for components with extended lifetimes. The DExg model's ability to capture heavy-tailed behavior further enhances its applicability in reliability analysis. By accommodating various failure patterns, it aids in developing effective maintenance strategies and risk assessments, particularly in safety-critical fields such as electronics, mechanical systems, and industrial applications. Thus, the DExg distribution is a powerful tool for enhancing system's reliability in both series and parallel configurations.

3.5. The mean (in)active time function

The mean active time (MAT) function for discrete random variables measures the expected remaining lifetime of a system or component, given that it has survived up to a certain point. It is a key tool in reliability analysis and survival studies, helping us to understand the future performance of a system after reaching a specific time. In contrast, the mean inactive time (MIT) function focuses on the average duration the system or component has already lasted before a certain time point. Both the MAT and MIT functions are crucial for assessing the lifetime behavior of discrete random variables, with applications in fields like actuarial science, medical studies, and industrial reliability testing. For complex models like the DExg distribution, both the MAT and MIT can be derived in explicit forms, although their expressions may be quite elaborate. Simplifications occur in special cases, such as when the parameter ζ approaches 0 or ∞, providing clearer insights into the probabilistic behavior of the model. The MAT, say $\kappa(i)$, for the DExg distribution can be represented as follows:

$$\begin{aligned}\kappa(i) &= E(Z-i|Z\geq i);\ i=0,1,2,3,...\\ &= \frac{1}{\Pr(Z\geq i;\zeta,\tau)}\sum_{z=i}^{\infty}(z-i)\Pr(Z=z;\zeta,\tau)\\ &= \begin{cases} \frac{1}{e^{\tau}-1} & ;\quad \zeta\to 0\\ \frac{\tau^2\left(\left[i^2+2i+1\right]e^{2\tau}-\left[2i^2+2i-1\right]e^{\tau}+i^2\right)+2\tau\left([i+1]e^{2\tau}-[2i+1]e^{\tau}+i\right)+2\left(e^{2\tau}-2e^{\tau}+1\right)}{\tau^2\left(i^2e^{3\tau}-3i^2e^{2\tau}+3i^2e^{\tau}-i^2\right)+2\tau\left(ie^{3\tau}-3ie^{2\tau}+3ie^{\tau}-i\right)+2\left(e^{3\tau}-3e^{2\tau}+3e^{\tau}-1\right)} & ;\quad \zeta\to\infty. \end{cases}\end{aligned}$$

Similarly, the MIT, say $\kappa^*(i)$, for the DExg model can be formulated as follows:

$$\begin{aligned}\kappa^*(i) &= E(i-Z|Z\leq i);\ \kappa^*(0)=0\\ &= \begin{cases} \frac{\left(ie^{\tau(i+1)}-[i+1]e^{i\tau}+1\right)e^{\tau}}{\left(e^{\tau(i+1)}-1\right)(e^{\tau}-1)} & ;\quad \zeta\to 0\\ \frac{A(i,\tau)}{B(i,\tau)} & ;\quad \zeta\to\infty, \end{cases}\end{aligned}$$

where

$$\begin{aligned}A(i,\tau) &= \tau^2\left(\left[2i+i^2+1\right]e^{3\tau}-e^{\tau(i+3)}-\left[2i^2+2i-1\right]e^{2\tau}-e^{\tau(i+2)}+i^2e^{\tau}\right)\\ &+2\tau\left([i+1]e^{3\tau}-[2i+1]e^{2\tau}-e^{\tau(i+3)}+e^{\tau(i+2)}+ie^{\tau}\right)\\ &+2\left(ie^{\tau(i+4)}-[1+3i]e^{\tau(i+3)}+[2+3i]e^{\tau(i+2)}-[1+i]e^{\tau(i+1)}+e^{3\tau}-2e^{2\tau}+e^{\tau}\right),\end{aligned}$$

and

$$\begin{aligned}B(i,\tau) &= \tau^2\left(\left[-i^2-2i-1\right]e^{3\tau}+3\left[2i+i^2+1\right]e^{2\tau}-3\left[i^2+2i+1\right]e^{\tau}+i^2+2i+1\right)\\ &+2\tau\left([i+1]\left[-e^{3\tau}+3e^{2\tau}-3e^{\tau}\right]+i\right)\\ &+2\left(e^{\tau(i+4)}-3e^{\tau(i+3)}+3e^{\tau(i+2)}-e^{\tau(i+1)}-e^{3\tau}+3e^{2\tau}-2e^{\tau}+1\right).\end{aligned}$$

Table 3 lists some numerical calculations for the MAT and MIT discussed in this section.

Table 3. The MAT and MIT utilizing the DExg distribution.

Measure	$\zeta \downarrow \tau \rightarrow$	0.1	0.3	0.5	0.7	0.9	1.5	5.0	10.0
MAT	0.5	21.4064	4.7669	2.2653	1.3568	0.9057	0.3588	0.0081	0.00005
	0.7	21.4335	4.7783	2.2707	1.3599	0.9077	0.3595	0.0082	0.00005
	0.9	21.4486	4.7846	2.2738	1.3616	0.9088	0.3599	0.0082	0.00005
MIT	0.5	3.1422	4.7246	6.3986	7.6900	8.5075	9.4929	9.9908	9.99993
	0.7	3.0431	4.5407	6.1623	7.4690	8.3339	9.4258	9.9899	9.99993
	0.9	2.9849	4.4279	6.0066	7.3113	8.2009	9.3672	9.9890	9.99993

Table 3 illustrates how the two measures, MAT and MIT, change in response to variations in the parameters ζ and τ when utilizing the DExg distribution. The distribution demonstrates sensitivity to both parameters, with significant changes in behavior depending on their specific combination. For MAT, as τ increases while ζ remains constant, the values tend to decrease, indicating a quicker approach to equilibrium or progressively shorter absolute times approaching zero. Conversely, for MIT, with ζ held constant, increasing τ results in values that rise and eventually stabilize around 10, signifying a longer interarrival time.

4. Various estimation approaches

4.1. Maximum likelihood estimation (MLE)

Consider a random sample $Z_1, Z_2, \ldots, Z_m$ drawn from the DExg model. The log-likelihood function (L) for the DExg distribution can be written as

$$L(\underline{z}|\zeta,\tau) = n\log\left(\frac{\zeta\tau^2}{\zeta+\tau^2}\right) - \tau\sum_{j=1}^{m} z_j + \sum_{j=1}^{m}\log\left[\eta\left(z_j;\zeta,\tau\right) - e^{-\tau}\eta\left(z_j+1;\zeta,\tau\right)\right]. \tag{4.1}$$

Taking the derivative of the log-likelihood with respect to the parameters ζ and τ and equating it to zero, we get the normal equations in the following form

$$\frac{n\tau^2}{\zeta\left(\zeta+\tau^2\right)} - \frac{1}{\zeta^2}\sum_{j=1}^{m}\frac{1+e^{-\tau}}{\eta\left(z_j;\zeta,\tau\right) - e^{-\tau}\eta\left(z_j+1;\zeta,\tau\right)} = 0,$$

$$\frac{2n\zeta}{\tau\left(\zeta+\tau^2\right)} - \sum_{j=1}^{m} z_j + \sum_{j=1}^{m}\frac{-2\tau^{-3} - z_j\tau^{-2} - \left[e^{-\tau}\left(-2\tau^{-3} - (z_j+1)\tau^{-2}\right) - \eta\left(z_j+1;\zeta,\tau\right)e^{-\tau}\right]}{\eta\left(z_j;\zeta,\tau\right) - e^{-\tau}\eta\left(z_j+1;\zeta,\tau\right)} = 0,$$

respectively. An analytical solution for this equation cannot be obtained; thus, a numerical iterative method must be employed using R software. In our study, we estimate the parameters ζ and τ of the DExg distribution using the *optim*() function from the base *stats* package. The optimization is performed by defining the negative log-likelihood function and minimizing it to obtain the best-fitting parameter estimates. Given the flexibility and efficiency of *optim*(), it is a suitable choice for our model's parameter estimation. For more complex likelihood models, *mle*2() from *bbmle* or *maxLik*() from *maxLik* could provide alternative approaches with more optimization techniques and statistical diagnostics.

4.2. Weighted (least-squares) estimators

Consider a random sample from the DExg model, with the order statistics $Z_{(1)}, Z_{(2)}, \cdots, Z_{(m)}$. The least-squares estimator (LSE) of the DExg parameters, denoted $\widehat{\zeta}_{LS}$ and $\widehat{\tau}_{LS}$, can be reported by solving the non-linear equation defined as follows:

$$\sum_{j=1}^{m}\left[1-\frac{\zeta\tau^2 e^{-\tau(z_{(j)}+1)}}{\zeta+\tau^2}\eta\left(z_{(j)}+1;\zeta,\tau\right)-\frac{j}{m+1}\right]\Delta_r\left(z_{(j)}|\zeta,\tau\right)=0;\ r=1,2, \tag{4.2}$$

with respect to the parameters ζ and τ, where

$$\begin{aligned}\Delta_1\left(z_{(j)}|\zeta,\tau\right)&=\frac{\partial}{\partial\zeta}F\left(z_{(j)}|\zeta,\tau\right)=\frac{\tau^2 e^{-\tau(z_{(j)}+1)}}{(\zeta+\tau^2)}\left[\frac{1}{\zeta}-\frac{\tau^2\eta\left(z_{(j)}+1;\zeta,\tau\right)}{(\zeta+\tau^2)}\right],\\ \Delta_2\left(z_{(j)}|\zeta,\tau\right)&=\frac{\partial}{\partial\tau}F\left(z_{(j)}|\zeta,\tau\right)=\frac{\zeta\tau^2 e^{-\tau(z_{(j)}+1)}\left(2\tau^{-3}+(z_{(j)}+1)\tau^{-2}\right)}{\zeta+\tau^2}+\eta\left(z_{(j)}+1;\zeta,\tau\right)\\ &\quad\times\frac{e^{-\tau(z_{(j)}+1)}\left[\left(\zeta+\tau^2\right)\zeta\left[\tau^2(z_{(j)}+1)+2\tau\right]+2\zeta\tau^3\right]}{\left(\zeta+\tau^2\right)^2}.\end{aligned} \tag{4.3}$$

Note that the solution of $\Delta_r\left(z_{(j)}|\zeta,\tau\right)=0;\ r=1,2$ can be obtained numerically. The weighted LSE (WLSE), say $\widehat{\zeta}_{WLS}$ and $\widehat{\tau}_{WLS}$, can be derived by solving the non-linear equation defined by

$$\sum_{j=1}^{m}\frac{(m+1)^2(m+2)}{j(m-j+1)}\left[1-\frac{\zeta\tau^2 e^{-\tau(z_{(j)}+1)}}{\zeta+\tau^2}\eta\left(z_{(j)}+1;\zeta,\tau\right)-\frac{j}{m+1}\right]\Delta_r\left(z_{(j)}|\zeta,\tau\right)=0;\ r=1,2, \tag{4.4}$$

with respect to the parameters ζ and τ, where $\Delta_r\left(z_{(j)}|\zeta,\tau\right)$ is defined in Eq (4.3). To estimate the parameters ζ and τ of theDExg model using LSE and WLSE, we rely on solving the nonlinear equations numerically. Several R packages provide robust tools for this task. The *nleqslv* package is particularly effective for solving nonlinear systems, allowing direct computation of the estimators by finding the roots of the equations. Similarly, the *rootSolve* package offers an alternative multivariate root-finding approach. When direct root-finding is challenging, the *optim* function from the *stats* package can be used to minimize the squared sum of the LSE or WLSE equations, transforming the problem into an optimization framework. These numerical techniques ensure the accurate and efficient estimation of ζ and τ for the DExg model. By incorporating weighted adjustments in WLSE, we account for heteroscedasticity and improve the estimations' reliability. These methods have been applied in our study to obtain the best-fitting parameter values, enhancing the model's applicability to real-world data analysis.

4.3. Anderson–Darling and right–tail Anderson–Darling estimators

Assume a random sample $Z_1, Z_2, \ldots, Z_m$ drawn from the DExg distribution. The Anderson-Darling estimator (ADE) is another type of minimum distance estimator. The ADE of the DExg parameters, say $\widehat{\zeta}_{AD}$ and $\widehat{\tau}_{AD}$, are derived by minimizing

$$AD(\zeta,\tau)=-m-\frac{1}{m}\sum_{j=1}^{m}(2j-1)\left[\begin{array}{c}\log\left\{1-\frac{\zeta\tau^2 e^{-\tau(z_{(j)}+1)}}{\zeta+\tau^2}\eta\left(z_{(j)}+1;\zeta,\tau\right)\right\}\\ +\log\left\{\frac{\zeta\tau^2 e^{-\tau(z_{(j)}+1)}}{\zeta+\tau^2}\eta\left(z_{(j)}+1;\zeta,\tau\right)\right\}\end{array}\right]. \tag{4.5}$$

Concerning the parameters ζ and τ, the model is subject to optimization, while the right–tail Anderson-Darling estimator (RADE) of the model parameter is achieved through minimization

$$RAD(\zeta,\tau) = \frac{m}{2} - 2\sum_{j=1}^{m}\left\{1 - \frac{\zeta\tau^2 e^{-\tau(z_{(j:m)}+1)}}{\zeta+\tau^2}\eta\left(z_{(j:m)}+1;\zeta,\tau\right)\right\} - \frac{1}{m}\sum_{j=1}^{m}(2j-1)\left[\log\left\{\frac{\zeta\tau^2 e^{-\tau(z_{(m+1-j:m)}+1)}}{\zeta+\tau^2}\eta\left(z_{(m+1-j:m)}+1;\zeta,\tau\right)\right\}\right], \tag{4.6}$$

with respect to the parameters ζ and τ. To solve the ADE and RADE for the DExg model in R, numerical optimization can be performed using packages such as *optim*(), *nlminb*(), *DEoptim*, or *GenSA* to minimize the respective objective functions with respect to the parameters ζ and τ. In our study, the *optim*() function is applied for the numerical optimization of the objective functions.

4.4. Maximum product of spacings estimator (MPSE)

In this section, we explore the estimation of the DExg parameters using the MPSE method with a complete sample. Consider a random sample $Z_1, Z_2, \ldots, Z_n$ drawn from the DExg distribution. For $j = 1, 2, \ldots, m+1$, let

$$W_j(\zeta,\tau) = \frac{\zeta\tau^2 e^{-\tau(z_{(j-1)}+1)}}{\zeta+\tau^2}\eta\left(z_{(j-1)}+1;\zeta,\tau\right) - \frac{\zeta\tau^2 e^{-\tau(z_{(j)}+1)}}{\zeta+\tau^2}\eta\left(z_{(j)}+1;\zeta,\tau\right),$$

be the uniform spacings of a random sample from the DExg distribution, where $F\left(z_{(0)}|\zeta,\tau\right) = 0$, $F\left(z_{(m+1)}|\zeta,\tau\right) = 1$, and $\sum_{j=1}^{m+1} W_j(\zeta,\tau) = 1$. The MPSE of ζ and τ, say $\widehat{\zeta}_{MPS}$ and $\widehat{\tau}_{MPS}$, can be derived by maximizing the geometric mean of the spacings

$$V(\zeta,\tau) = \left[\prod_{j=1}^{m+1}\left\{\frac{\zeta\tau^2 e^{-\tau(z_{(j-1)}+1)}}{\zeta+\tau^2}\eta\left(z_{(j-1)}+1;\zeta,\tau\right) - \frac{\zeta\tau^2 e^{-\tau(z_{(j)}+1)}}{\zeta+\tau^2}\eta\left(z_{(j)}+1;\zeta,\tau\right)\right\}\right]^{\frac{1}{m+1}}, \tag{4.7}$$

with respect to the parameters ζ and τ. In R, the MPSE can be computed using multiple approaches, although there is no specific built-in function for this purpose. Instead, optimization functions such as *optim*(), *nlm*(), or *nlminb*() can be utilized to determine the MPSE by maximizing the product of the spacings, which is equivalent to minimizing the negative logarithm of the spacings' product. In our study, we employed the *optim*() function to estimate the parameters ζ and τ of the DExg distribution. The optimization was performed by defining an appropriate objective function based on the negative log-product of spacings, allowing us to obtain accurate estimates for ζ and τ that had the best fit to the observed data.

4.5. Cramer–Von–Mises estimator (CVME)

The CVME represents the difference between the estimated CDF and the empirical CDF. To estimate the CVME of the DExg parameters, one must solve the following non–linear equation:

$$\sum_{j=1}^{m}\left[1 - \frac{\zeta\tau^2 e^{-\tau(z_{(j)}+1)}}{\zeta+\tau^2}\eta\left(z_{(j)}+1;\zeta,\tau\right) - \frac{2j-1}{2m}\right]\Delta_r\left(z_{(j)}|\zeta,\tau\right) = 0, \tag{4.8}$$

with respect to the parameters ζ and τ, where $\Delta_r\left(z_{(j)}|\zeta,\tau\right)$ is defined in Equation (4.3). To solve this equation numerically in R, optimization techniques such as *optim*() or *nlminb*() can be applied, where the objective function is defined by the sum of the weighted differences between the estimated CDF and the empirical CDF, using the relevant expressions for $\Delta_r\left(z_{(j)}|\zeta,\tau\right)$.

4.6. Percentile estimator (PCE)

Let $w_j = j/(m+1)$ be an unbiased estimator of $F\left(z_{(j)}|\zeta,\tau\right)$. Hence, the PCE of the parameter β, denoted by $\widehat{\zeta}_{PC}$ and $\widehat{\tau}_{PC}$, can be reported by minimizing

$$P(\zeta,\tau) = \sum_{j=1}^{m}\left(z_{(j)} - D\left(w_j\right)\right)^2,$$

with respect to the parameters ζ and τ, where $D\left(w_j\right) = F^{-1}\left(z_{(j)}|\zeta,\tau\right)$ is the quantile function of the DExg model. To solve for ζ and τ, we can use numerical optimization in R, specifically utilizing packages like *optim*() or *nlminb*(), to minimize the sum of squared differences between the observed data $z_{(j)}$ and the predicted quantiles $D\left(w_j\right)$.

5. Simulation ranking techniques

Simulation ranking techniques are a powerful tool for evaluating and comparing the performance of different statistical estimators or models. The process begins by generating a large number of simulated datasets, typically using known parameter values or distributions, which allows researchers to test estimators under controlled conditions. Various estimation methods, such as MPSE, ADE, MLE, LSE, RADE, PCE, CVME, and WLSE, are applied to these datasets to estimate the model parameters. The performance of each estimator is then evaluated by calculating error metrics like bias (the difference between the true and estimated parameters), mean squared error (MSE), and mean relative error (MRE), which quantify how accurately the estimators recover the true values. Once these error metrics are computed, the estimators are ranked according to their performance, with the estimator showing the smallest error metrics being considered the best. The process is typically repeated across a large number of simulation replications (e.g., 10,000 or more samples) to account for variability and ensure that the results are not due to random fluctuations. Simulation ranking techniques are particularly useful when dealing with complex models or when analytical solutions for comparing estimators are not feasible. They provide robust and comprehensive insights into the strengths and weaknesses of different estimation methods under various conditions, such as varying sample sizes, different parameter settings, or specific data characteristics.

In this section, we evaluate the effectiveness of MPSE, ADE, MLE, LSE, RADE, PCE, CVME, and WLSE in relation to the sample size n using R software with DExg parameters, where a random variable Z is generated from the DExg distribution by discretizing a value X drawn from a continuous distribution, followed by Markov Chain Monte Carlo (MCMC) simulations, with a simulation study involving the generation of $N = 10,000$ samples across four schemes with different parameter settings ζ and τ (Scheme I: $\zeta = 0.5$, $\tau = 0.2$; Scheme II: $\zeta = 0.2$, $\tau = 0.4$; Scheme III: $\zeta = 0.4$, $\tau = 0.2$; Scheme IV: $\zeta = 0.2$, $\tau = 0.5$) with varying sample sizes ($n_1 = 20$, $n_2 = 50$, $n_3 = 150$, $n_4 = 300$), and

the computation of the estimators and error metrics such as bias, MSE, MRE for these samples, where

$$|\text{Bias}(\epsilon)| = \frac{1}{N}\sum_{k=1}^{N}\left|\widehat{\epsilon_k} - \epsilon_k\right|, \ \ \text{MSE}(\epsilon) = \frac{1}{N}\sum_{k=1}^{N}(\widehat{\epsilon_k} - \epsilon_k)^2, \ \text{MRE}(\epsilon) = \frac{1}{N}\sum_{k=1}^{N}\frac{\left|\widehat{\epsilon_k} - \epsilon_k\right|}{\epsilon_k}.$$

Table 4. Simulation results of Scheme I.

n	Est	Par	ML	WLS	PC	RAD	MPS	AD	CVM	OLS
20	$\|Bias\|$	$\widehat{\zeta}$	0.1686_1	0.1933_4	0.2130_6	0.2162_7	0.1942_5	0.2269_8	0.1722_2	0.1816_3
		$\widehat{\tau}$	0.2971_2	0.2978_3	0.3537_6	0.3660_7	0.3026_4	0.4430_8	0.2942_1	0.3467_5
	MSE	$\widehat{\zeta}$	0.0280_1	0.0369_4	0.0447_6	0.0461_7	0.0372_5	0.0292_2	0.0508_8	0.0325_3
		$\widehat{\tau}$	0.0871_2	0.0875_3	0.1234_6	0.1321_7	0.0903_4	0.1937_8	0.0854_1	0.1186_5
	MRE	$\widehat{\zeta}$	0.3373_1	0.3867_4	0.4260_6	0.4325_7	0.3885_5	0.4539_8	0.3444_2	0.3632_3
		$\widehat{\tau}$	0.1981_2	0.1985_3	0.2358_6	0.2440_7	0.2017_4	0.2953_8	0.1961_1	0.2311_5
Sum of ranks			9_1	21_3	36_6	$42_{7.5}$	27_5	$42_{7.5}$	15_2	24_4
50	$\|Bias\|$	$\widehat{\zeta}$	0.1070_1	0.1183_4	0.1310_6	0.1312_7	0.1198_5	0.1518_8	0.1145_2	0.1172_3
		$\widehat{\tau}$	0.1857_1	0.1895_2	0.2113_5	0.2207_7	0.1898_3	0.3379_8	0.1915_4	0.2131_6
	MSE	$\widehat{\zeta}$	0.0113_1	0.0138_3	0.0168_6	0.0169_7	0.0141_4	0.0227_8	0.0129_2	0.0157_5
		$\widehat{\tau}$	0.0340_1	0.0354_2	0.0441_6	0.0480_7	0.0355_3	0.1127_8	0.0362_4	0.0450_5
	MRE	$\widehat{\zeta}$	0.2141_1	0.2367_4	0.2621_6	0.2624_7	0.2396_5	0.3036_8	0.2291_2	0.2345_3
		$\widehat{\tau}$	0.1238_1	0.1263_2	0.1409_5	0.1471_7	0.1265_3	0.2253_8	0.1277_4	0.1424_6
Sum of ranks			6_1	17_2	34_6	42_7	23_4	48_8	18_3	27_5
150	$\|Bias\|$	$\widehat{\zeta}$	0.0595_1	0.0641_3	0.0758_7	0.0748_6	0.0665_4	0.0878_8	0.0624_2	0.0675_5
		$\widehat{\tau}$	0.1021_1	0.1091_2	0.1238_6	0.1228_5	0.1156_4	0.2160_8	0.1108_3	0.1278_7
	MSE	$\widehat{\zeta}$	0.0035_1	0.0040_3	0.0056_7	0.0055_6	0.0043_4	0.0076_8	0.0038_2	0.0045_5
		$\widehat{\tau}$	0.0102_1	0.0117_2	0.0151_6	0.0149_5	0.0132_4	0.0460_8	0.0121_3	0.0161_7
	MRE	$\widehat{\zeta}$	0.1191_1	0.1283_3	0.1517_7	0.1497_6	0.1330_4	0.1757_8	0.1246_2	0.1351_5
		$\widehat{\tau}$	0.0680_1	0.0727_2	0.0825_6	0.0819_5	0.0771_4	0.1440_8	0.0739_3	0.0853_7
Sum of ranks			6_1	$15_{2.5}$	39_7	33_5	24_4	48_8	$15_{2.5}$	36_6
300	$\|Bias\|$	$\widehat{\zeta}$	0.0417_1	0.0446_2	0.0501_6	0.0506_7	0.0482_5	0.0643_8	0.0470_4	0.0464_3
		$\widehat{\tau}$	0.0726_1	0.0727_2	0.0829_5	0.0852_6	0.0772_4	0.1630_8	0.0766_3	0.0891_7
	MSE	$\widehat{\zeta}$	0.0017_1	0.0019_2	0.0024_6	0.0025_7	0.0022_5	0.0040_8	0.0020_3	0.0021_4
		$\widehat{\tau}$	0.0052_1	0.0053_2	0.0068_5	0.0071_6	0.0059_4	0.0262_8	0.0057_3	0.0078_7
	MRE	$\widehat{\zeta}$	0.0834_1	0.0891_2	0.1002_6	0.1012_7	0.0964_5	0.1286_8	0.0940_4	0.0928_3
		$\widehat{\tau}$	0.0485_1	0.0491_2	0.0553_5	0.0568_6	0.0515_4	0.1087_8	0.0510_3	0.0594_7
Sum of ranks			6_1	12_2	33_6	39_7	27_4	48_8	20_3	31_5

Table 5. Simulation results of Scheme II.

n	Est	Par	ML	WLS	PC	RAD	MPS	AD	CVM	OLS
20	$\lvert Bias\rvert$	$\widehat{\zeta}$	0.1390_1	0.1536_5	0.1627_7	0.1622_6	0.1480_4	0.1789_8	0.1399_2	0.1425_3
		$\widehat{\tau}$	0.6749_2	0.6769_3	0.7474_6	0.7282_5	0.7020_4	0.9389_8	0.6621_1	0.7806_7
	MSE	$\widehat{\zeta}$	0.0190_1	0.0233_5	0.0261_7	0.0259_6	0.0216_4	0.0316_8	0.0193_2	0.0208_3
		$\widehat{\tau}$	0.4495_2	0.4522_3	0.5512_6	0.5233_5	0.4863_4	0.8698_8	0.4325_1	0.6013_7
	MRE	$\widehat{\zeta}$	0.2778_1	0.3073_5	0.3254_7	0.3244_6	0.2960_4	0.3579_8	0.2799_2	0.2850_3
		$\widehat{\tau}$	0.2249_2	0.2256_3	0.2491_6	0.2427_5	0.2340_4	0.3129_8	0.2207_1	0.2602_7
Sum of ranks			$9_{1.5}$	$24_{3.5}$	39_7	33_6	$24_{3.5}$	48_8	$9_{1.5}$	30_5
50	$\lvert Bias\rvert$	$\widehat{\zeta}$	0.0818_1	0.0946_4	0.0996_6	0.1027_7	0.0900_2	0.1235_8	0.0910_3	0.0964_5
		$\widehat{\tau}$	0.4025_1	0.4360_4	0.4797_6	0.4691_5	0.4247_2	0.6564_8	0.4276_3	0.4884_7
	MSE	$\widehat{\zeta}$	0.0066_1	0.0088_4	0.0098_6	0.0104_7	0.0080_2	0.0150_8	0.0081_3	0.0091_5
		$\widehat{\tau}$	0.1599_1	0.1875_4	0.2271_6	0.2171_5	0.1780_2	0.4252_8	0.1804_3	0.2354_7
	MRE	$\widehat{\zeta}$	0.1637_1	0.1893_4	0.1993_6	0.2054_7	0.1801_2	0.2468_8	0.1820_3	0.1929_5
		$\widehat{\tau}$	0.1341_1	0.1453_4	0.1599_6	0.1564_5	0.1415_2	0.2188_8	0.1425_3	0.1628_7
Sum of ranks			6_1	24_4	36_6	36_6	12_2	48_8	18_3	36_6
150	$\lvert Bias\rvert$	$\widehat{\zeta}$	0.0503_1	0.0504_2	0.0587_7	0.0580_6	0.0530_3	0.0714_8	0.0536_4	0.0561_5
		$\widehat{\tau}$	0.2284_1	0.2361_2	0.2695_5	0.2753_6	0.2539_4	0.4279_8	0.2519_3	0.2770_7
	MSE	$\widehat{\zeta}$	0.0024_1	0.0025_2	0.0033_7	0.0032_6	0.0027_3	0.0050_8	0.0028_4	0.0031_5
		$\widehat{\tau}$	0.0514_1	0.0551_2	0.0717_5	0.0748_6	0.0636_4	0.1807_8	0.0626_3	0.0757_7
	MRE	$\widehat{\zeta}$	0.1005_1	0.1008_2	0.1173_7	0.1161_6	0.1060_3	0.1429_8	0.1073_4	0.1123_5
		$\widehat{\tau}$	0.0761_1	0.0787_2	0.0898_4	0.0917_6	0.0846_5	0.1426_8	0.0839_3	0.0923_7
Sum of ranks			6_1	12_2	35_5	$36_{6.5}$	22_4	48_8	21_3	$36_{6.5}$
300	$\lvert Bias\rvert$	$\widehat{\zeta}$	0.0340_1	0.0361_3	0.0412_6	0.0417_7	0.0371_4	0.0536_8	0.0351_2	0.0398_5
		$\widehat{\tau}$	0.1641_1	0.1691_3	0.1930_6	0.1880_5	0.1700_4	0.3195_8	0.1686_2	0.2075_7
	MSE	$\widehat{\zeta}$	0.0011_1	0.0013_3	0.0016_6	0.0018_7	0.0014_4	0.0028_8	0.0012_2	0.0015_5
		$\widehat{\tau}$	0.0265_1	0.0282_3	0.0367_6	0.0348_5	0.0285_4	0.1007_8	0.0280_2	0.0425_7
	MRE	$\widehat{\zeta}$	0.0680_1	0.0722_3	0.0824_6	0.0835_7	0.0742_4	0.1074_8	0.0703_2	0.0797_5
		$\widehat{\tau}$	0.0551_1	0.0563_3	0.0643_6	0.0626_5	0.0567_4	0.1065_8	0.0562_2	0.0691_7
Sum of ranks			6_1	18_3	36_6	36_6	24_4	48_8	12_2	36_6

Table 6. Simulation results of Scheme III.

n	Est	Par	ML	WLS	PC	RAD	MPS	AD	CVM	OLS
20	$\|Bias\|$	$\widehat{\zeta}$	0.3292_1	0.3857_5	0.4281_6	0.4040_8	0.3719_3	0.4286_7	0.3422_2	0.3820_4
		$\widehat{\tau}$	0.7623_3	0.7620_2	0.8743_5	0.8846_7	0.7690_4	0.9842_8	0.7594_1	0.8835_6
	MSE	$\widehat{\zeta}$	0.1069_1	0.1468_5	0.1808_7	0.1610_6	0.1364_3	0.1812_8	0.1155_2	0.1440_4
		$\widehat{\tau}$	0.5731_3	0.5729_2	0.7542_7	0.7723_6	0.5835_4	0.9559_8	0.5691_1	0.7702_5
	MRE	$\widehat{\zeta}$	0.2194_1	0.2571_5	0.2854_7	0.2693_6	0.2479_3	0.2857_8	0.2281_2	0.2546_4
		$\widehat{\tau}$	0.2540_3	0.2539_2	0.2914_5	0.2948_7	0.2563_4	0.3280_8	0.2531_1	0.2945_6
Sum of ranks			12_2	$21_{3.5}$	37_6	40_7	$21_{3.5}$	47_8	9_1	29_5
50	$\|Bias\|$	$\widehat{\zeta}$	0.2085_1	0.2143_3	0.2453_7	0.2444_6	0.2181_4	0.2889_8	0.2131_2	0.2335_5
		$\widehat{\tau}$	0.4461_1	0.4726_2	0.5346_5	0.5431_6	0.4941_4	0.6950_8	0.4738_3	0.5436_7
	MSE	$\widehat{\zeta}$	0.0429_1	0.0453_3	0.0594_7	0.0589_6	0.0469_4	0.0824_8	0.0448_2	0.0538_5
		$\widehat{\tau}$	0.1964_1	0.2204_2	0.2820_5	0.2910_6	0.2409_4	0.4767_8	0.2215_3	0.2915_7
	MRE	$\widehat{\zeta}$	0.1390_1	0.1428_3	0.1635_7	0.1629_6	0.1454_4	0.1926_8	0.1420_2	0.1556_5
		$\widehat{\tau}$	0.1487_1	0.1575_2	0.1782_5	0.1810_6	0.1647_4	0.2316_8	0.1579_3	0.1812_7
Sum of ranks			6_1	$15_{2.5}$	36_6	36_6	24_4	48_8	$15_{2.5}$	36_6
150	$\|Bias\|$	$\widehat{\zeta}$	0.1167_1	0.1251_2	0.1324_6	0.1374_7	0.1266_3	0.1715_8	0.1282_4	0.1294_5
		$\widehat{\tau}$	0.2512_1	0.2681_2	0.3112_6	0.3018_5	0.2761_3	0.4472_8	0.2794_4	0.3151_7
	MSE	$\widehat{\zeta}$	0.0134_1	0.0154_2	0.0173_6	0.0186_7	0.0159_3	0.0289_8	0.0162_4	0.0165_5
		$\widehat{\tau}$	0.0622_1	0.0709_2	0.0955_6	0.0899_5	0.0752_3	0.1973_8	0.0770_4	0.0979_7
	MRE	$\widehat{\zeta}$	0.0778_1	0.0833_2	0.0883_6	0.0916_7	0.0844_3	0.1141_8	0.0854_4	0.0862_5
		$\widehat{\tau}$	0.0837_1	0.0893_2	0.1037_6	0.1006_5	0.0920_3	0.1491_8	0.0931_4	0.1050_7
Sum of ranks			6_1	12_2	36_6	36_6	18_3	48_8	24_4	36_6
300	$\|Bias\|$	$\widehat{\zeta}$	0.0848_2	0.0834_1	0.0984_6	0.1007_7	0.0892_4	0.1244_8	0.0854_3	0.0944_5
		$\widehat{\tau}$	0.1790_1	0.1887_3	0.2159_5	0.2229_6	0.1967_4	0.3182_8	0.1878_2	0.2307_7
	MSE	$\widehat{\zeta}$	0.0071_2	0.0068_1	0.0095_6	0.0100_7	0.0078_4	0.0289_8	0.0072_3	0.0088_5
		$\widehat{\tau}$	0.0316_1	0.0351_3	0.0460_5	0.0490_6	0.0382_4	0.1973_8	0.0348_2	0.0525_7
	MRE	$\widehat{\zeta}$	0.0565_2	0.0556_1	0.0656_6	0.0671_7	0.0595_4	0.0829_8	0.0569_3	0.0629_5
		$\widehat{\tau}$	0.0596_1	0.0629_3	0.0719_5	0.0743_6	0.0655_4	0.1060_8	0.0626_2	0.0769_7
Sum of ranks			9_1	12_2	33_5	39_7	24_5	48_8	15_4	36_6

Table 7. Simulation results of Scheme IV.

n	Est	Par	ML	WLS	PC	RAD	MPS	AD	CVM	OLS
20	$\|Bias\|$	$\widehat{\zeta}$	0.5605_1	0.6249_5	0.7053_7	0.6967_6	0.6098_4	0.7396_8	0.5623_2	0.5862_3
		$\widehat{\tau}$	0.0939_3	0.0937_2	0.1035_5	0.1062_7	0.0923_1	0.1745_8	0.0950_4	0.1053_6
	MSE	$\widehat{\zeta}$	0.3102_1	0.3853_6	0.0316_2	0.4790_7	0.3670_5	0.5398_8	0.3120_3	0.3391_4
		$\widehat{\tau}$	0.0087_3	0.0086_2	0.0098_5	0.0111_7	0.0084_1	0.0300_8	0.0089_4	0.0110_6
	MRE	$\widehat{\zeta}$	0.3738_1	0.4167_5	0.4702_7	0.4645_6	0.4065_4	0.4931_8	0.3748_2	0.3908_3
		$\widehat{\tau}$	0.1878_3	0.1874_2	0.2069_5	0.2125_7	0.1846_1	0.3490_8	0.1900_4	0.2106_6
Sum of ranks			12_1	22_4	31_6	40_7	16_2	48_8	19_3	28_5
50	$\|Bias\|$	$\widehat{\zeta}$	0.3514_1	0.3840_4	0.4216_6	0.4279_7	0.3975_5	0.5035_8	0.3659_2	0.3700_3
		$\widehat{\tau}$	0.0570_1	0.0604_3	0.0654_6	0.0629_5	0.0608_4	0.1328_8	0.0581_2	0.0678_7
	MSE	$\widehat{\zeta}$	0.1218_1	0.1455_4	0.1678_6	0.1807_7	0.1560_5	0.2501_8	0.1321_2	0.1351_3
		$\widehat{\tau}$	0.0031_1	0.0036_3	0.0044_6	0.0039_5	0.0037_4	0.0174_8	0.0033_2	0.0045_7
	MRE	$\widehat{\zeta}$	0.2342_1	0.2560_4	0.2810_6	0.2852_7	0.2650_5	0.3356_8	0.2439_2	0.2467_3
		$\widehat{\tau}$	0.1134_1	0.1209_3	0.1308_6	0.1260_5	0.1216_4	0.2656_8	0.1161_2	0.1357_7
Sum of ranks			6_1	21_3	$36_{6.5}$	$36_{6.5}$	27_4	48_8	12_2	30_5
150	$\|Bias\|$	$\widehat{\zeta}$	0.1967_1	0.2099_3	0.2621_7	0.2434_6	0.2257_5	0.3166_8	0.2156_4	0.2031_2
		$\widehat{\tau}$	0.0316_1	0.0325_2	0.0382_7	0.0352_4	0.0343_3	0.0856_8	0.0353_5	0.0365_6
	MSE	$\widehat{\zeta}$	0.0381_1	0.0434_3	0.1753_8	0.0584_6	0.0502_5	0.0989_7	0.0459_4	0.0407_2
		$\widehat{\tau}$	0.0009_1	0.0010_2	0.0042_7	0.0014_6	0.0012_4	0.0072_8	0.0011_3	0.0013_5
	MRE	$\widehat{\zeta}$	0.1311_1	0.1400_3	0.1747_7	0.1623_6	0.1505_5	0.2111_8	0.1437_4	0.1354_2
		$\widehat{\tau}$	0.0633_1	0.0651_2	0.0764_7	0.0704_4	0.0686_3	0.1714_8	0.0705_5	0.0731_6
			6_1	15_2	43_7	32_6	$25_{4.5}$	47_8	$25_{4.5}$	23_3
300	$\|Bias\|$	$\widehat{\zeta}$	0.1367_1	0.1470_3	0.1791_6	0.1833_7	0.1502_4	0.2230_8	0.1532_5	0.1461_2
		$\widehat{\tau}$	0.0228_1	0.0243_4	0.0284_7	0.0266_5	0.0233_2	0.0641_8	0.0239_3	0.0267_6
	MSE	$\widehat{\zeta}$	0.0184_1	0.0213_3	0.4909_7	0.0331_6	0.0222_4	0.0490_8	0.0231_5	0.0210_2
		$\widehat{\tau}$	0.0003_1	0.0006_4	0.0105_8	0.0007_5	0.0004_2	0.0040_7	0.0005_3	0.0009_6
	MRE	$\widehat{\zeta}$	0.0912_1	0.0980_3	0.1194_6	0.1225_7	0.1001_4	0.1487_8	0.1020_5	0.0974_2
		$\widehat{\tau}$	0.0457_1	0.0487_4	0.0569_7	0.0531_5	0.0467_2	0.1283_8	0.0479_3	0.0534_6
Sum of ranks			6_1	21_3	41_7	35_6	18_2	47_8	$24_{4.5}$	$24_{4.5}$

Table 8. Ranking of the estimation methods based on the simulation results.

	n	ML	WLS	PC	RAD	MPS	AD	CVM	OLS
Scheme I	20	1	3	6	7.5	5	7.5	2	4
	50	1	2	6	7	4	8	3	5
	150	1	2.5	7	5	4	8	2.5	6
	300	1	2	6	7	4	8	3	5
Scheme II	20	1.5	3.5	7	6	3.5	8	1.5	5
	50	1	4	6	6	2	8	3	6
	150	1	2	5	6.5	4	8	3	6.5
	300	1	3	6	6	4	8	2	6
Scheme III	20	2	3.5	6	7	3.5	8	1	5
	50	1	2.5	6	6	4	8	2.5	6
	150	1	2	6	6	3	8	4	6
	300	1	2	5	7	5	8	4	6
Scheme IV	20	1	4	6	7	2	8	13	5
	50	1	3	6.5	6.5	4	8	2	5
	150	1	2	7	6	4.5	8	4.5	3
	300	1	3	7	6	2	8	4.5	4.5
Sum of ranks		17.5	44	98.5	102.5	58.5	127.5	45.5	84
Mean of ranks		1.09	2.75	6.16	6.41	3.66	7.97	2.84	5.25
SD of ranks		0.27	0.73	0.63	0.64	0.96	0.13	1.03	0.91
Overall rank		1	2	6	7	4	8	3	5

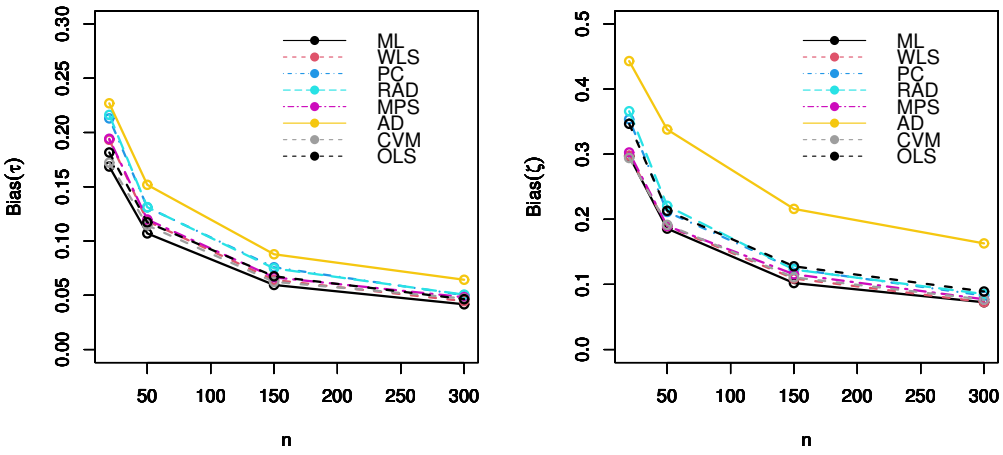

Figure 4. The bias of the estimation methods for Scheme I.

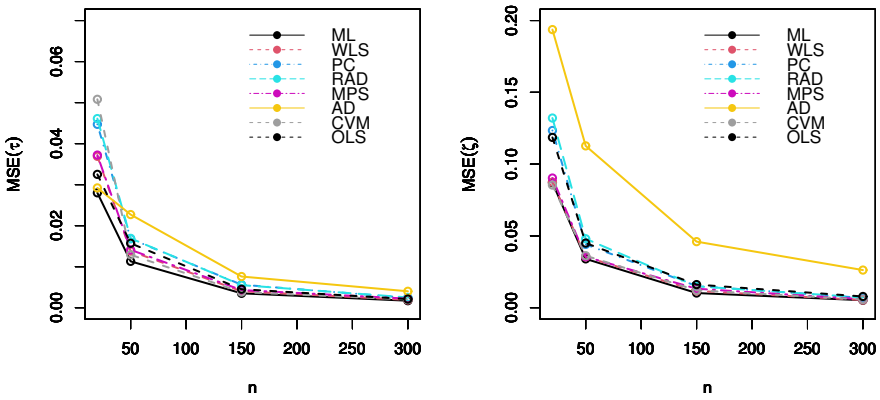

Figure 5. The MSE of the estimation methods for Scheme I.

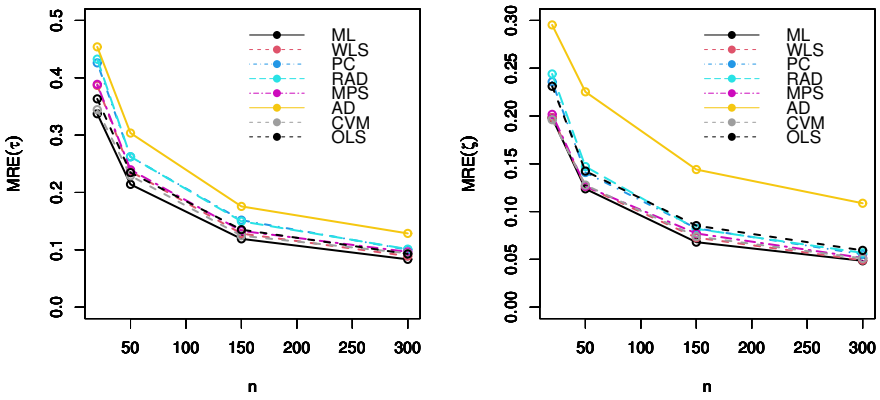

Figure 6. The MRE of the estimation methods for Scheme I.

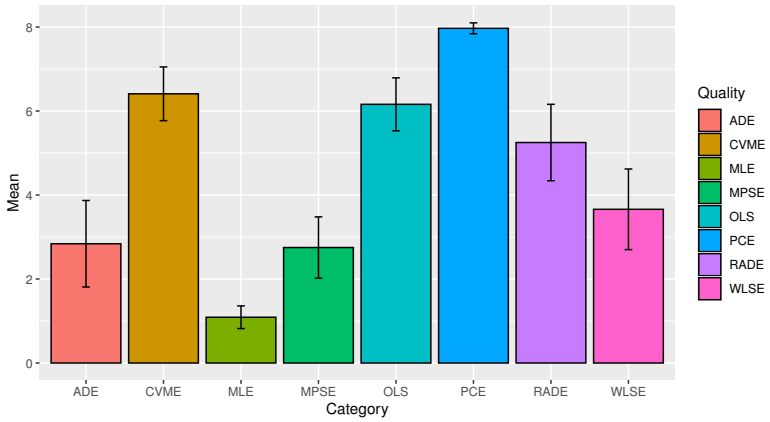

Figure 7. The mean and standard deviation of the ranks for the different estimation methods.

The MSE measures the average squared difference between the predicted and actual values, with a lower MSE indicating that predictions are closer to the actual values. In contrast, the MRE represents the average relative difference as a percentage, providing insights into accuracy and normalization across different data magnitudes. While the MSE emphasizes precision by squaring errors, the MRE considers the relative size of the errors. The MSE can be sensitive to outliers, whereas the MRE may be less affected when expressed in percentage terms. Although the MSE is less interpretable due to its squared units, the MRE offers a standardized measure of error as a percentage. The choice between MSE and MRE depends on the characteristics of the data and whether the focus is on precision or accuracy in the predictions. The empirical results from the simulation are presented in Tables 4–8 and Figures 4–7.

From Tables 4 to 7, it is clear that as the sample size n increases, the bias of the parameters ζ and τ decreases, approaching zero. Similarly, both the MSE and MRE of the DExg parameters improve as the sample size grows, indicating the reliability of the estimators. Additionally, all estimation methods perform well across various sample sizes. As shown in Table 8 and Figure 7, the MLE method stands out as the top performer, achieving the lowest rank across the sum of ranks, mean of ranks, standard deviation of ranks, and overall rank. This highlights MLE as the most effective method among the ones tested.

6. Data analysis: goodness-of-fit

Within this section, we demonstrate the flexibility of the DExg distribution in effectively modeling diverse datasets across different fields. The fitted distributions are evaluated by employing the Chi-square (χ^2) test along with its associated P–value. The distribution that provided the best fit was chosen on the basis of the lowest χ^2 statistic and the highest P-value. A low P–value (typically below 0.05) indicates a poor fit, while a high P–value suggests a good fit between the observed data and the fitted distribution. The fit of the DExg distribution is compared with those of other competing distributions, including the discrete inverted Nadarajah–Haghighi (DINH), discrete inverse Weibull (DIW), discrete Burr Type II (DBX–II), geometric (Geo), Poisson (Poi), discrete Pareto (DPa), discrete Rayleigh (DR), and discrete inverse Rayleigh (DIR).

6.1. Radiation biology data: application in biotechnology

Radiation biology data, including studies on agents like streptonigrin, examines the effects of radiation and radiation-like substances on living organisms. Streptonigrin, a genotoxic agent, induces DNA damage and cytogenetic lesions, making it a valuable tool for studying cellular responses to stress. These data are essential for understanding mechanisms like DNA repair, apoptosis, and mutagenesis caused by such agents. It also aids in developing targeted cancer therapies and radioprotective agents to minimize damage to healthy tissues. By integrating biological research with biotechnology, the study of substances like streptonigrin enhances our understanding of genotoxicity and its applications in medicine and environmental safety. In this section, the dataset, referred to as "Dataset I", pertains to mammalian cytogenetic dosimetry, specifically examining lesions in rabbit lymphoblasts induced by the genotoxic agent streptonigrin (NSC-45383). The exposure level for the study was set at 60 μg/kg. This dataset provides insights into the cytogenetic effects of streptonigrin, offering a basis for understanding its impact on cellular structures and functions. For a detailed

description of the experimental setup and findings, refer to the study by Shanker and Fesshaye [24]. Figure 8 illustrates the distribution of the data, which exhibits a right-skewed asymmetry. This skewness is attributed to the presence of several extreme observations that influence the overall distribution. Additionally, the data shows a unimodal shape, characterized by a single peak. The distribution is platykurtic, meaning it has a flatter peak and lighter tails compared with a normal distribution. Furthermore, there is evidence of overdispersion, indicating that the variance exceeds the mean, suggesting that the data's variability is higher than expected under a standard model.

Table 9 presents the results of the goodness-of-fit test for Dataset I, evaluating the performance of several statistical models applied to the data. The models considered include the DExg, DB-XII, and Geo models. Figure 9 visually supports these empirical results, highlighting how each model fits the observed data. The figure compares the predictions from each model with the actual data, providing a clear view of the discrepancies and overall fit. While all three models are capable of modeling the data, the DExg model stands out as the most effective, offering the best fit and demonstrating superior accuracy in capturing the distribution of the data. Furthermore, Figure 10 proves the uniqueness property of the model estimators, confirming that the parameter estimates derived from the DExg model are stable and uniquely determined for the given dataset. This figure further reinforces the reliability of the DExg model, making it the most suitable choice for this analysis. Together, Table 9, Figure 9, and Figure 10 provide a thorough assessment of the model's performance, with the DExg model being identified as the optimal choice for Dataset I.

Table 9. The goodness–of–fit test for Dataset I.

X	OF	DExg	DINH	DIW	DB-XII	Geo	Poi	DPa	DR	DIR
0	413	413.29	414.58	411.60	412.71	407.68	374.05	447.06	273.43	411.86
1	124	123.96	91.62	136.59	132.73	131.14	177.38	84.54	274.53	134.96
2	42	41.61	31.37	29.13	33.25	42.18	42.06	29.96	50.49	29.47
3	15	14.52	15.79	10.39	11.29	13.57	6.65	13.99	2.515	10.68
4	5	5.05	9.50	4.82	4.79	4.36	0.79	7.66	0.04	5.01
5	0	1.72	6.34	2.61	2.36	1.40	0.07	4.64	0.00	2.74
6	2	0.84	31.80	5.86	3.87	0.67	0.00	13.15	0.00	6.28
Total		601	601	601	601	601	601	601	601	601
$-l$		556.197	595.708	564.056	560.131	556.516	582.677	580.141	700.860	564.095
MLE_{ζ}		0.198	23.1217	0.684	0.187	0.322	0.474	0.140	0.545	0.685
MLE_{τ}		1.363	0.0137	2.041	1.653	–	–	–	–	–
χ^2		0.069	51.489	12.234	5.563	0.660	58.562	39.711	156.05	11.861
d.f		2	4	3	2	3	3	4	1	4
P–value		0.966	< 0.001	0.007	0.062	0.883	< 0.001	< 0.001	< 0.001	0.018

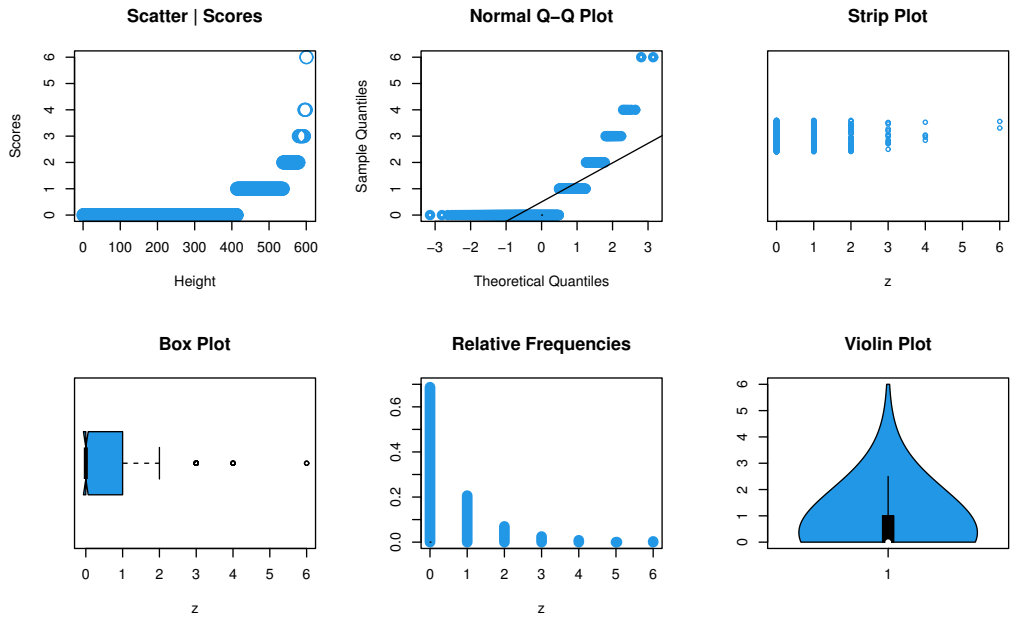

Figure 8. Non–parametric plots for Dataset I.

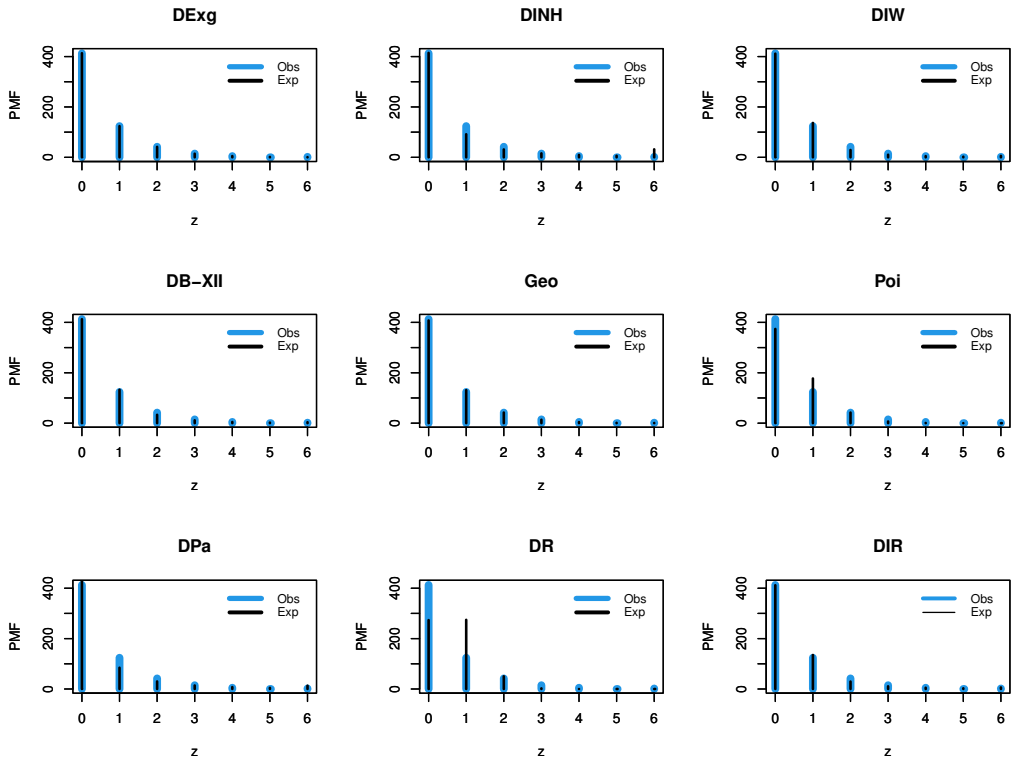

Figure 9. The estimated PMF based on Dataset I.

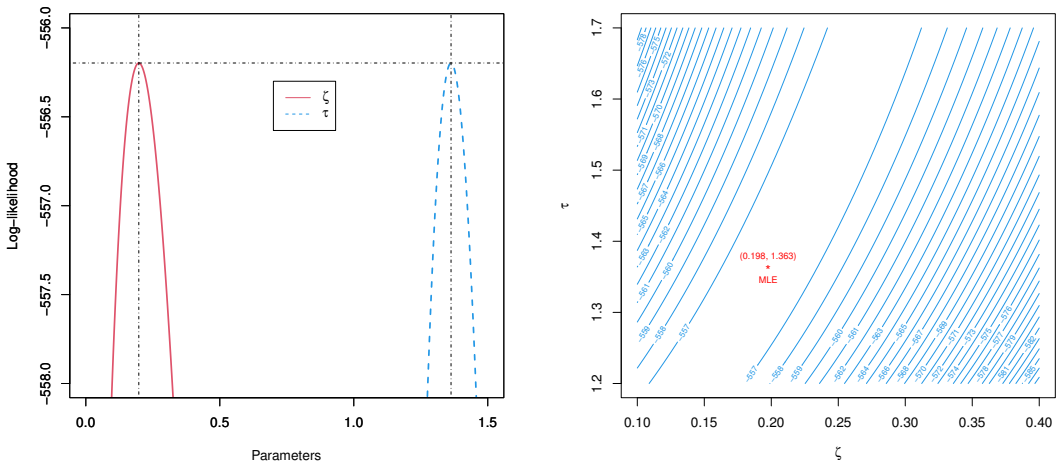

Figure 10. The log-likelihood profiles based on Dataset I.

Table 10 displays the estimation techniques applied to Dataset I, highlighting various methods used to estimate the model parameters. It is evident that all of the methods can be applied to the data; however, the MLE stands out as the most effective approach.

Table 10. Various estimators for Dataset I.

	ML	MPS	OLS	WLS	CVM	PC	AD	RAD
$\widehat{\zeta}$	0.198	0.192	0.195	0.196	0.194	0.186	0.187	0.189
$\widehat{\tau}$	1.363	1.371	1.331	1.358	1.371	1.412	1.284	1.295
χ^2	0.069	0.134	0.484	0.078	0.117	1.545	2.319	1.764
d.f	2	2	2	2	2	2	2	2
P.value	0.966	0.935	0.785	0.962	0.943	0.462	0.314	0.414

6.2. Modeling breakdown counts over time: application in industrial engineering

Industrial engineering focuses on optimizing complex systems and processes to improve efficiency and productivity across various industries. It involves analyzing workflows, reducing waste, and ensuring that resources are utilized in the most effective way possible. One key aspect of industrial engineering is the management of machines' performance, where engineers monitor and address issues such as computer breakdowns occurring over a period. These breakdowns can disrupt production schedules and lead to downtime, which significantly impacts overall productivity. Industrial engineers use predictive maintenance strategies and data analysis to anticipate equipment failures, minimizing downtime and improving the reliability of manufacturing systems. This section presents a dataset that records the number of computer breakdowns occurring over a span of 128 consecutive weeks of operation (see Hand et al. [25]). Figure 11 illustrates the distribution of Dataset II. The results reveal a moderate rightward skew, likely due to the presence of some extreme observations, along with a relatively high level of variability. The kurtosis indicates that the distribution has slightly heavier tails than a normal distribution, though not excessively so, and shows

evidence of overdispersion.

Table 11 presents the results of the goodness–of–fit test for Dataset II, assessing the performance of various statistical models applied to the data, including the DExg and Geo models. Figure 12 visually complements these results, illustrating how each model fits the observed data by comparing their predictions to the actual data and highlighting any discrepancies and the overall fit. While all three models are capable of modeling the data, the DExg model stands out as the most effective, providing the best fit and demonstrating superior accuracy in capturing the data's distribution. Additionally, Figure 13 confirms the uniqueness property of the model estimators, showing that the parameter estimates derived from the DExg model are stable and uniquely determined for the given dataset. This further emphasizes the reliability of the DExg model, establishing it as the most suitable choice for this analysis. Together, Table 11, Figure 9, and Figure 13 offer a comprehensive evaluation of the models' performance, with the DExg model identified as the optimal choice for Dataset II.

Table 11. The goodness–of–fit test for Dataset II.

X	OF	DExg	DINH	DIW	DB-XII	Geo	Poi	DPa	DR	DIR
0	15	19.04	12.40	9.69	19.89	25.53	2.31	47.81	3.64	3.24
1	19	16.47	30.16	33.09	36.59	20.43	9.27	19.19	10.30	47.81
2	23	16.06	19.94	23.10	19.05	16.36	18.61	10.76	15.31	34.02
3	14	15.23	12.78	14.48	10.69	13.09	24.91	7.02	18.04	16.65
4	15	13.61	8.72	9.54	6.83	10.49	25.01	5.00	18.44	8.77
5	10	11.52	6.29	6.64	4.76	8.39	20.09	3.77	16.92	5.08
6	8	9.33	4.73	4.84	3.52	6.72	13.44	2.97	14.17	3.17
7	4	7.28	3.69	3.65	2.72	5.38	7.71	2.40	10.94	2.11
8	6	5.52	2.95	2.85	2.17	4.31	3.87	1.99	7.84	1.47
9	2	4.09	2.41	2.27	1.77	3.46	1.74	1.69	5.23	1.06
10	3	2.97	2.01	1.85	1.48	2.75	0.69	1.45	3.26	0.79
11	3	2.12	1.69	1.53	1.25	2.21	0.25	1.26	1.89	0.60
12	2	1.49	1.46	1.28	1.08	1.77	0.08	1.11	1.04	0.47
+13	4	3.27	18.758	13.183	16.188	7.114	0.006	21.586	0.985	2.762
Total	128	128	128	128	128	128	128	128	128	128
$-l$		318.953	331.931	330.446	342.581	320.703	384.974	369.766	347.148	356.525
MLE_{ζ}		0.497	1.244	0.076	0.785	0.801	4.016	0.509	0.972	0.025
MLE_{τ}		0.513	1.634	1.235	3.309	–	–	–	–	–
χ^2		7.093	20.199	18.709	40.183	11.651	88.995	94.971	49.897	50.533
d.f		8	6	6	5	9	6	6	8	5
P–value		0.527	0.003	0.005	0	0.234	0	0	0	0

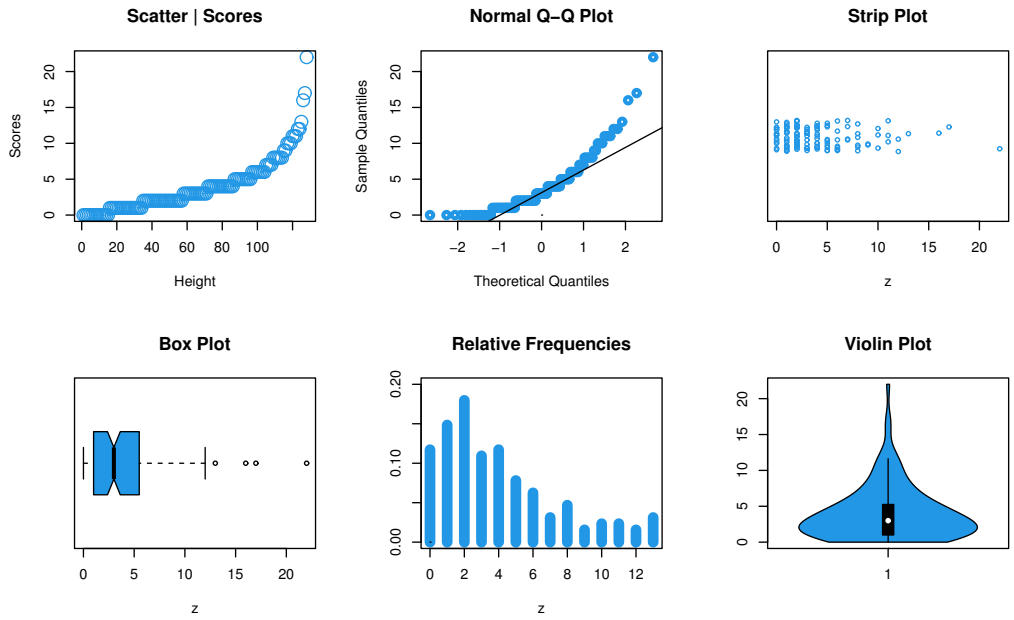

Figure 11. Non–parametric plots for Dataset II.

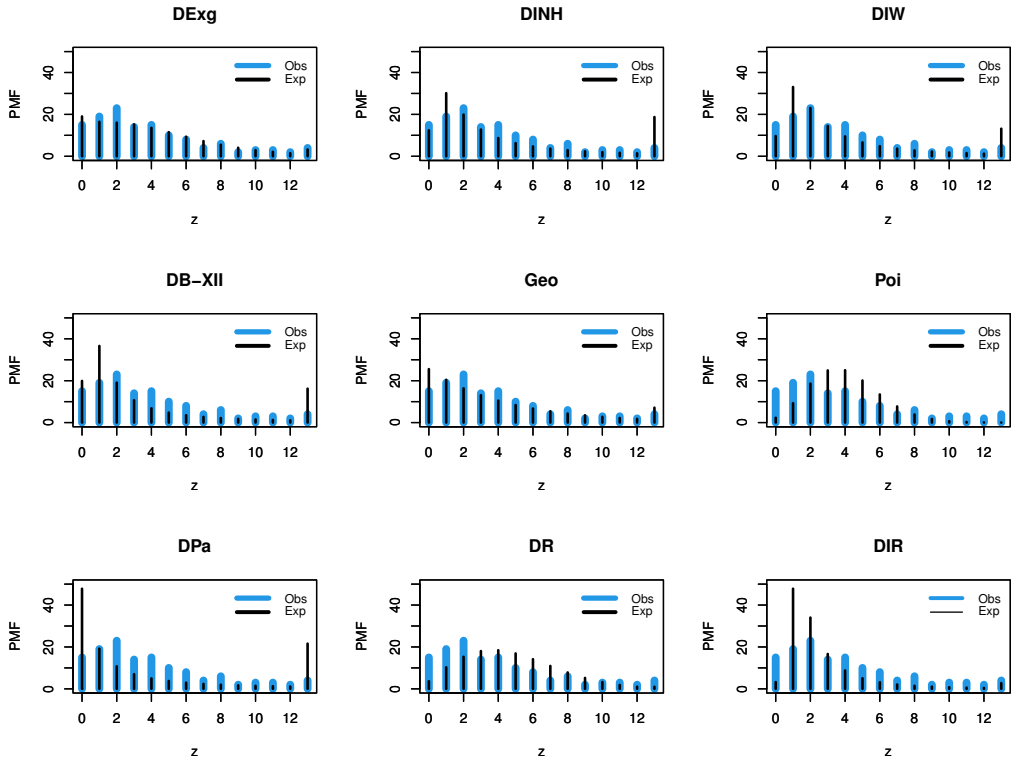

Figure 12. The estimated PMF for Dataset II.

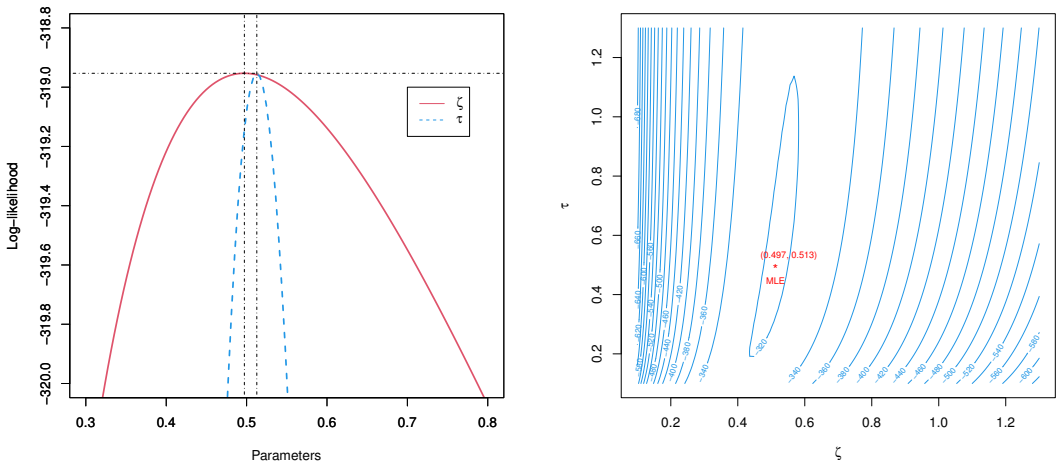

Figure 13. The log–likelihood profiles based on Dataset II.

Table 12 presents the estimation techniques applied to Dataset II, showcasing the different methods used to estimate the model parameters. While all methods are applicable to the data, the MLE emerges as the most effective approach.

Table 12. Numerical descriptors for characterizing the DExg distribution.

	ML	MPS	OLS	WLS	CVM	PC	AD	RAD
$\widehat{\zeta}$	0.497	0.474	0.513	0.483	0.495	0.461	0.501	0.526
$\widehat{\tau}$	0.513	0.522	0.532	0.512	0.522	0.527	0.582	0.565
χ^2	7.093	7.831	7.932	7.683	7.711	8.153	10.766	11.0434
d.f	8	8	8	8	8	8	7	8
P.value	0.527	0.450	0.440	0.465	0.462	0.419	0.149	0.199

6.3. Application of the DExg model in radiation biology and industrial engineering: modeling, prediction, and risk management

The DExg distribution proves to be a highly suitable and effective model for both radiation biology and industrial engineering applications due to its flexibility and ability to accommodate complex features in data.

For the radiation biology dataset, the DExg distribution excels in modeling data with skewness, overdispersion, zero–inflation, and heavy tails, which are common in radiation studies. These characteristics make it more adaptable to the irregularities found in radiation exposure data, where the majority of observations might cluster around a certain value with occasional extreme readings. The ability to handle overdispersion, where the variance exceeds the mean, and to effectively model rare, extreme events (heavy tails) provides a better fit compared with simpler models such as the normal or exponential distributions. As a result, the DExg distribution allows for a more accurate representation of biological processes and better risk assessments regarding radiation exposure.

In industrial engineering, particularly in the prediction and prevention of machine breakdowns, the DExg distribution's ability to model failure times under variable conditions is crucial. Machines typically follow a lifetime distribution that is skewed, with a few units experiencing early failures, while the majority last longer, making it challenging to predict breakdowns with simple models. The DExg distribution's flexibility to model skewed data and handle overdispersion makes it ideal for modeling the time-to-failure data of machines in industrial settings. By effectively capturing the nuances of machines' breakdown behavior, the DExg distribution enables predictive maintenance, reducing downtime and maintenance costs while improving the reliability and efficiency of industrial systems.

In both fields, the DExg distribution not only enhances predictive accuracy but also provides valuable insights for risk management and decision-making. Its application helps in optimizing resources, scheduling maintenance, and improving systems' reliability, ensuring that both radiation biology studies and industrial operations achieve better outcomes through the application of advanced statistical modeling techniques. Thus, the DExg distribution stands as a powerful tool in both the biological and industrial domains, offering practical solutions to complex data modeling challenges.

7. Conclusions and future work

In this paper, the DExg model was introduced, with several key objectives aimed at addressing practical challenges in count data analysis. The model offers a discrete distribution with simple and closed-form solutions for fundamental properties, such as the probability mass function, cumulative distribution function, moments, and others. It was designed to be highly applicable to real-world datasets, including those from industrial and mortality studies, which exhibit bathtub–, or increasing failure rates. Moreover, the DExg model was crafted to accommodate a wide range of data types, such as equi–, over–, and under–dispersed datasets, as well as those with positive skewness or leptokurtic distributions. Various estimation strategies were explored, and through simulations and a ranking methodology, the maximum likelihood estimation method was identified as the most effective. Two distinct datasets from biotechnology and industrial engineering were analyzed, with the proposed model demonstrating superior fit compared with alternative models. Notably, the DExg model outperformed several well-established discrete models in the current statistical literature, further underscoring its robustness and applicability. Future work will focus on extending the model for forecasting and bivariate analysis, as well as performing a sensitivity analysis to assess the impact of model misspecification.

Author contributions

Conceptualization, Mohamed S. Eliwa; data curation, Mahmoud El-Morshedy and Mohamed S. Algolam; formal analysis, Mohamed S. Eliwa, Mohamed S. Algolam and Mohamed El-Dawoody; investigation, Mahmoud El-Morshedy and Mohamed S. Algolam; methodology, Mahmoud El-Morshedy and Mohamed S. Eliwa; resources, Mohamed S. Algolam and Mohamed El-Dawoody; software, Mahmoud El-Morshedy and Mohamed S. Eliwa; validation, Mohamed S. Eliwa and Mohamed El-Dawoody; writing–review and editing, Mahmoud El-Morshedy and Mohamed S. Eliwa. All authors have read and agreed to the published version of the manuscript.

Use of Generative-AI tools declaration

The authors declare they have not used AI tools in the creation of this article.

Acknowledgments

The authors extend their appreciation to Prince Sattam bin Abdulaziz University for funding this research work through the project number (PSAU/2024/01/31935).

Conflict of interest

The authors declare that they have no conflicts of interest.

References

1. J. Melnikow, A. Padovani, M. Miller, Frontline physician burnout during the COVID-19 pandemic: national survey findings, *BMC Health Serv. Res.*, **22** (2022), 365. https://doi.org/10.1186/s12913-022-07728-6
2. J. Mapes, Using big data to study small places: small-town voting patterns in the 2020 US presidential election, *Growth Change*, **55** (2024), e12730. https://doi.org/10.1111/grow.12730
3. E. Clough, T. Barrett, S. E. Wilhite, P. Ledoux, C. Evangelista, I. F. Kim, et al., NCBI GEO: archive for gene expression and epigenomics data sets: 23-year update, *Nucleic Acids Res.*, **52** (2024), D138–D144. https://doi.org/10.1093/nar/gkad965
4. S. Yang, D. Meng, A. Díaz, H. Yang, X. Su, A. M. D. Jesus, Probabilistic modeling of uncertainties in reliability analysis of mid-and high-strength steel pipelines under hydrogen-induced damage, *Int. J. Struct. Integr.*, **16** (2025), 39–59. https://doi.org/10.1108/IJSI-10-2024-0177
5. S. Yang, D. Meng, H. Yang, C. Luo, X. Su, Enhanced soft Monte Carlo simulation coupled with support vector regression for structural reliability analysis, In: *Proceedings of the Institution of Civil Engineers-Transport*, Emerald Publishing Limited, 2024, 1–16. https://doi.org/10.1680/jtran.24.00128
6. D. Meng, H. Yang, S. Yang, Y. Zhang, A. M. De Jesus, J. Correia, et al., Kriging-assisted hybrid reliability design and optimization of offshore wind turbine support structure based on a portfolio allocation strategy, *Ocean Eng.*, **295** (2024), 116842. https://doi.org/10.1016/j.oceaneng.2024.116842
7. S. Sen, S. K. Ghosh, H. Al-Mofleh, The Mirra distribution for modeling time-to-event data sets, In: *Dtrategic management, decision theory, and decision science: contributions to policy issues*, Singapore: Springer, 2021. https://doi.org/10.1007/978-981-16-1368-5_5
8. D. Roy, Discrete Rayleigh distribution, *IEEE Trans. Reliab.*, **53** (2004), 255–260. https://doi.org/10.1109/TR.2004.829161
9. M. El-Morshedy, M. S. Eliwa, E. Altun, Discrete Burr-Hatke distribution with properties, estimation methods and regression model, *IEEE Access*, **8** (2020), 74359–74370. https://doi.org/10.1109/ACCESS.2020.2988431

10. H. Krishna, P. S. Pundir, Discrete Burr and discrete Pareto distributions, *Stat. Methodol.*, **6** (2009), 177–188. https://doi.org/10.1016/j.stamet.2008.07.001
11. T. Hussain, M. Ahmad, Discrete inverse Rayleigh distribution, *Pakistan J. Stat.*, **30** (2014).
12. A. E. Abd EL-Hady, M. A. Hegazy, A. A. EL-Helbawy, A discrete exponentiated generalized family of distributions, *Comput. J. Math. Stat. Sci.*, **2** (2023), 303–327.
13. A. R. E. Alosey, A. M. Gemeay, A novel version of geometric distribution: method and application, *Comput. J. Math. Stat. Scie.*, **4** (2025), 1–16.
14. M. A. Jazi, C. D. Lai, M. H. Alamatsaz, A discrete inverse Weibull distribution and estimation of its parameters, *Stat. Methodol.*, **7** (2010), 121–132. https://doi.org/10.1016/j.stamet.2009.11.001
15. E. Gómez-Déniz, E. Calderín-Ojeda, The discrete Lindley distribution: properties and applications, *J. Stat. Comput. Simul.*, **81** (2011), 1405–1416. https://doi.org/10.1080/00949655.2010.487825
16. J. M. Jia, Z. Z. Yan, X. Y. Peng, A new discrete extended Weibull distribution, *IEEE Access*, **7** (2019), 175474–175486. https://doi.org/10.1109/ACCESS.2019.2957788
17. E. Altun, A new generalization of geometric distribution with properties and applications, *Commun. Stat.-Simul. Comput.*, **49** (2020), 793–807. https://doi.org/10.1080/03610918.2019.1639739
18. E. Gómez-Déniz, Another generalization of the geometric distribution, *Test*, **19** (2010), 399–415. https://doi.org/10.1007/s11749-009-0169-3
19. M. A. Hegazy, R. E. Abd El-Kader, A. A. El-Helbawy, G. R. Al-Dayian, Bayesian estimation and prediction of discrete Gompertz distribution, *J. Adv. Math. Comput. Sci.*, **36** (2021), 1–21.
20. V. Nekoukhou, M. H. Alamatsaz, H. Bidram, Discrete generalized exponential distribution of a second type, *Statistics*, **47** (2013), 876–887. https://doi.org/10.1080/02331888.2011.633707
21. A. S. Eldeeb, M. Ahsan-ul-Haq, M. S. Eliwa, A discrete Ramos-Louzada distribution for asymmetric and over-dispersed data with leptokurtic-shaped: properties and various estimation techniques with inference, *AIMS Math.*, **7** (2022), 1726–1741. https://doi.org/10.3934/math.2022099
22. T. Hussain, M. Aslam, M. Ahmad, A two parameter discrete Lindley distribution, *Rev. Colomb. Estad.*, **39** (2016), 45–61.
23. B. C. Arnold, N. Balakrishnan, H. N. Nagaraja, *A first course in order statistics*, Society for Industrial and Applied Mathematics, 2008.
24. R. Shanker, H. Fesshaye, On Poisson-Sujatha distribution and its applications to model count data from biological sciences, *Biometrics Biostat. Int. J.*, **3** (2016), 1–7. https://doi.org/10.15406/bbij.2015.02.00036
25. D. J. Hand, F. Daly, K. McConway, D. Lunn, E. Ostrowski, *A handbook of small data sets*, Chapman & Hall, 1993. https://doi.org/10.1201/9780429246579